

ESEIAAT

*Bachelor's Thesis*



UNIVERSITAT POLITÈCNICA DE CATALUNYA  
BARCELONATECH

Escola Superior d'Enginyeries Industrial,  
Aeroespacial i Audiovisual de Terrassa

---

# **Sensitivity study of the implementation of Air-Breathing Electric Propulsion systems as atmospheric drag compensation measures Earth Observation CubeSat missions at Very Low Earth Orbits**

---

**BACHELOR'S THESIS**

**Degree: Bachelor's Degree in Aerospace Technologies Engineering**

**Delivery date: 30/09/2019**

**Student: Pau Nadal Vila**

**Director: Silvia Rodríguez Donaire**

**Co-Director: Miquel Sureda Anfres**



# Abstract

Placing a CubeSat in Very Low Earth Orbits can prove to be considerably beneficial for satellite imagery missions. To consistently benefit from its advantages though, any satellite in such orbits must compensate the drag force generated by the residual atmosphere or it will de-orbit in a matter of days. Any sort of thruster is therefore required. It can either be a conventional propulsion system with on-board stored fuel or an Air-Breathing Electric Propulsion system, which can collect its own fuel from the residual atmosphere.

This project evaluates the performance that both engines would have in a possible Very Low Earth Orbit Earth Observation scenario and discloses whether the Air-Breathing Electric Propulsion system can be a viable candidate as CubeSat drag compensation system with regards to conventional thrusters.

**Keywords:**

*Air-Breathing Electric Propulsion, CubeSat, Very Low Earth Orbit, Earth Observation, Satellite systems, Solar activity, Ion Engine, Field Emission Electric Propulsion, Drag compensation, Residual atmosphere, Small satellite*

# Acknowledgements

*To all coordinators of the DISCOVERER project: Silvia Rodríguez Donaire, Daniel García Almiñana and specially Miquel Sureda Anfres, for letting me take part in this project and for trying to help me even in quite difficult moments.*

*To all my friends, either from outside or inside the university, for all the the amazing experiences lived during those last four years.*

*To my family, for the unconditional support that they have given me during so many years of my life.*

# Honor Declaration

*I declare that,*

*the work in this Degree Thesis is completely my own work, no part of this Degree Thesis is taken from other people's work without giving them credit, all references have been clearly cited.*

*I understand that an infringement of this declaration leaves me subject to the foreseen disciplinary actions by The Universitat Politècnica de Catalunya-BarcelonaTECH.*

Title of the thesis: **Sensitivity study of the implementation of Air-Breathing Electric Propulsion systems as atmospheric drag compensation measures Earth Observation CubeSat missions at Very Low Earth Orbits**

Signed:

Pau Nadal Vila  
September 2019  
Bachelor's Degree in Aerospace Technologies Engineering



# Contents

<b>1</b>	<b>Introduction</b>	<b>11</b>
1.1	Aim . . . . .	11
1.2	Scope . . . . .	11
1.3	Requirements . . . . .	12
1.4	Justification . . . . .	12
<b>2</b>	<b>Background and State of the Art</b>	<b>13</b>
2.1	CubeSat state of the art . . . . .	13
2.2	Micro-propulsion systems state of the art . . . . .	15
2.3	ABEP and micro-ABEP state of the art . . . . .	16
2.3.1	ABEP designs review . . . . .	18
2.3.2	Air-Breathing Electrostatic Propulsion . . . . .	18
2.3.3	Air-Breathing Plasma Propulsion . . . . .	19
2.4	ABEP lifetime expectancy . . . . .	20
<b>3</b>	<b>Earth Orbits and physical environment</b>	<b>21</b>
3.1	Classification of Earth Orbits . . . . .	21
3.1.1	High Earth Orbits . . . . .	22
3.1.2	Medium Earth Orbits . . . . .	22
3.1.3	Low Earth Orbits . . . . .	23
3.1.3.1	Atmosphere model . . . . .	28
<b>4</b>	<b>Benefits and Challenges of orbiting in Low Earth Orbit</b>	<b>30</b>
4.1	Benefits and advantages . . . . .	30
4.2	Challenges and disadvantages . . . . .	31
<b>5</b>	<b>ABEP scenario proposal</b>	<b>32</b>
5.1	Scenario parameters . . . . .	32
5.1.1	Orbit proposal . . . . .	32
5.1.2	CubeSat conception . . . . .	33
5.1.3	Conventional propulsion power plant decision . . . . .	34
5.1.4	ABEP decision . . . . .	35
5.1.5	Adopted assumptions . . . . .	36
<b>6</b>	<b>CubeSat design using the IFM nano-thruster approach</b>	<b>38</b>
6.1	Structural architecture . . . . .	38
6.2	Systems and subsystems . . . . .	39
6.2.1	Payload system . . . . .	39
6.2.2	Attitude determination and control system . . . . .	40
6.2.2.1	Attitude sensors . . . . .	41
6.2.2.2	Attitude actuators . . . . .	42
6.2.3	Communication system . . . . .	43
6.2.4	Command and Data Handling system . . . . .	45
6.2.5	Thermal control system . . . . .	45

6.2.6	Propulsion system . . . . .	45
6.2.7	Electric power system . . . . .	47
6.3	Overall CubeSat system configuration . . . . .	49
6.3.1	Total mass budget . . . . .	49
6.3.2	Total power budget . . . . .	51
6.3.3	Total element budget . . . . .	54
6.3.4	CubeSat design conclusions . . . . .	56
<b>7</b>	<b>CubeSat design using ABEP approach</b>	<b>57</b>
7.1	Structural architecture . . . . .	57
7.2	Systems and subsystems . . . . .	57
7.2.1	Propulsion system . . . . .	58
7.2.2	ADCS . . . . .	59
7.2.3	Electric power system . . . . .	59
7.3	Overall CubeSat system configuration . . . . .	60
7.3.1	Total mass budget . . . . .	60
7.3.2	Total power budget . . . . .	61
7.3.3	Total element budget . . . . .	63
7.3.4	CubeSat design conclusions . . . . .	64
<b>8</b>	<b>CubeSat propulsion system performance analysis</b>	<b>65</b>
8.1	Drag force determination . . . . .	65
8.2	Propulsion operating altitude range determination . . . . .	67
8.3	Propulsion system operating lifetime . . . . .	68
<b>9</b>	<b>Environmental analysis</b>	<b>70</b>
<b>10</b>	<b>Conclusions</b>	<b>71</b>



# List of Figures

2.1	Small satellites classification [1] . . . . .	13
2.2	Physical and power typical constraints for <10kg CubeSats [2] . . . . .	13
2.3	Evolution of launched CubeSats over years[3] . . . . .	14
2.4	Decay time in orbit for various ballistic coefficients[4] . . . . .	15
2.5	Characteristics of current conventional micro-propulsion systems [5] . . . . .	16
2.6	ABEP concept [6] . . . . .	16
2.7	Intake Setups: (a) Funnel concept, (b) Bypass concept[7] . . . . .	18
2.8	ABEP classification . . . . .	19
3.1	Orbit Eccentricity[8] . . . . .	21
3.2	Orbit Inclination[9] . . . . .	22
3.3	Types of orbits according to altitude . . . . .	22
3.4	Molniya Orbit[9] . . . . .	23
3.5	Sun-synchronous circular orbits as function of altitude [10] . . . . .	24
3.6	Solar activity over time [11] . . . . .	25
3.7	Partial density of atmospheric species as a function of altitude[12] . . . . .	25
3.8	Average density of atomic oxygen as a function of altitude for minimum,nominal and maximum solar conditions[12] . . . . .	26
3.9	Comparison of different disturbing acceleration in LEO as function of altitude[4] . . . . .	26
3.10	Drag force as a function of altitude for different cross-sectional areas and in mean solar activity conditions[7] . . . . .	27
3.11	Variations of semi major axis and eccentricity as function of true anomaly during maximum solar activity (a-b) and minimum solar activity (c-d) for PRIRODA satellite[13] . . . . .	28
5.1	CubeSat orientation towards Earth . . . . .	34
5.2	Schematic representation of FEEP operation [14] . . . . .	35
5.3	Mock-up of the 6U AB-GIE thruster system [15] . . . . .	35
5.4	Schematic representation of ABEP operation [15] . . . . .	35
6.1	IFM nano-thruster relation between specific impulse, thrust and power consumption . . . . .	47
6.2	Relative mass distribution for CubeSat design using an IFM engine . . . . .	51
6.3	Relative power consumption in imaging mode for the IFM CubeSat design . . . . .	52
6.4	Relative power consumption in eclipse mode for the IFM CubeSat design . . . . .	53
6.5	Relative power consumption in downlink mode for the IFM CubeSat design . . . . .	53
6.6	Relative power consumption in battery recharge mode for the IFM CubeSat design . . . . .	54
6.7	Relative cost distribution for CubeSat design using an IFM engine . . . . .	55
7.1	Relative mass distribution for CubeSat design using the AB-GIE . . . . .	61
7.2	Relative power consumption in imaging mode for the AB-GIE CubeSat design . . . . .	62
7.3	Relative power consumption in eclipse mode for the AB-GIE CubeSat design . . . . .	62
7.4	Relative power consumption in downlink mode for the AB-GIE CubeSat design . . . . .	63

7.5	Relative power consumption in battery charge mode for the AB-GIE CubeSat design . . . . .	63
8.1	total atmospheric density as a function of altitude and for different levels of solar activity . . . . .	65
8.2	CubeSat's velocity a function of altitude . . . . .	66
8.3	Drag force as a function of altitude and solar activity . . . . .	67
8.4	Maximum available thrust for each propulsion system and its correlation to the drag force as a function of altitude and solar activity . . . . .	68

# List of Tables

3.1	Maximum, average and minimum solar and geomagnetic activity levels of the 2005-2016 solar cycle . . . . .	24
5.1	Reference orbit for the CubeSat conceptual design . . . . .	33
6.1	6U CubeSat structure parameters . . . . .	39
6.2	<i>Chameleon Imager</i> panchromatic camera parameters . . . . .	39
6.3	Current imaging resolution parameters . . . . .	40
6.4	Average disturbance torques acting on a 6U at 400km [16] . . . . .	41
6.5	Star tracker attitude sensor parameters . . . . .	41
6.6	Sun sensor parameters . . . . .	42
6.7	Reaction wheel parameters . . . . .	42
6.8	Magnetorquer parameters . . . . .	43
6.9	S-Band transmitter parameters . . . . .	43
6.10	S-Band antenna parameters . . . . .	44
6.11	UHF transceiver parameters . . . . .	44
6.12	UHF antenna parameters . . . . .	44
6.13	On-board computer parameters . . . . .	45
6.14	IFM nano-thruster parameters . . . . .	46
6.15	CubeSat summarised power budget for the several operation modes (without battery power consumption determined) and the IFM-design case . . . . .	48
6.16	Battery parameters . . . . .	48
6.17	Single BCT 6U solar panel parameters . . . . .	49
6.18	BCT 6U-H Triple Wing Solar Array parameters . . . . .	49
6.19	Mass budget for the CubeSat design using an IFM engine . . . . .	50
6.20	Power budget for the CubeSat design using an IFM engine . . . . .	52
6.21	Element budget for the CubeSat design using an IFM engine . . . . .	55
7.1	AB-GIE parameters . . . . .	58
7.2	AB-GIE parabolic air-intake . . . . .	58
7.3	Mass budget for the CubeSat design using an AB-GIE engine . . . . .	60
7.4	Power budget for the CubeSat design using an AB-GIE engine . . . . .	61
7.5	Element manufacture budget for the CubeSat design using an AB-GIE engine . . . . .	64
8.1	Minimum and maximum operating altitude of the AB-GIE system . . . . .	68
8.2	Minimum and maximum operating altitude of the IFM system . . . . .	68
8.3	IFM operating lifespan for the 3 different scenarios . . . . .	69
8.4	IFM operating lifespan for the 3 different scenarios and taking advantage of the spare mass . . . . .	69

# Chapter 1

## Introduction

### 1.1 Aim

The aim of this project is to estimate the performance that Air-Breathing Electric Propulsion (ABEP) systems should have so that they are a feasible option to compensate atmospheric drag in the case of Earth Observation (EO) CubeSats orbiting at Very Low Earth Orbit (VLEO).

### 1.2 Scope

In order to achieve the aim of this project, the following aspects will be addressed in this bachelor's thesis:

- General classification of orbits according to their altitude. Description of the very low earth orbit environment, its main characteristics and hazardous elements.
- Review of the most relevant low earth orbit operating benefits and challenges.
- Overall description of Air-Breathing Electric Propulsion systems.
- Estimation of the expected satellite lifespan increase due to Air-Breathing Electric Propulsion systems.
- Feasibility analysis of Air-Breathing Electric Propulsion systems CubeSats in Earth Observation missions.
- Environmental and risk analysis of Air-Breathing Electric Propulsion systems.

Nevertheless, the following points are considered out of the scope and will not be covered in this thesis.

- Technical design of any sort of propulsion system, including Air-Breathing Electric Propulsion ones.
- Exhaustive scientific data regarding atmosphere physical or chemical properties.
- Profound analysis of satellite capabilities.
- Satellite mission design or operating procedures.
- Detailed value chain analysis of satellite missions nor revenue models for satellite platforms.

### 1.3 Requirements

In order to fully tackle the project it has been delimited according to several restrictions, which are exposed below:

- The satellite's altitude has to be in between 160 to 450 km so that its orbit is considered as Very Low Earth Orbit[4].
- The satellite's tasks and functions have to be related with Earth Observation missions.
- The satellite approach will be that of a single monolithic spacecraft, rather than fractional architectures such as clusters or swarms.
- The satellite has to belong to the small satellite group known as CubeSats. Therefore, it has to follow the CubeSat Design specifications [17].
- For the feasibility analysis, the satellite itself can not carry a propulsion system other than an Air-Breathing Electric Propulsion system.

### 1.4 Justification

This bachelor's thesis is embedded into the European Union (EU) DISCOVERER project, funded by the EU Horizon 2020 research and innovation program. The DISCOVERER project aims to develop the key technologies required for a feasible operation of Earth Observation satellites operating at Low Earth Orbits. Furthermore, the project is an intent of a radical redesign of these satellites so that they become smaller and cheaper while still achieving the same or even better performance than nowadays satellite platforms[18].

Therefore, this specific bachelor's thesis focuses on the cost estimation of the Air-Breathing Electric Propulsion system that is being developed under the same DISCOVERER project as a drag compensation measure.

## Chapter 2

# Background and State of the Art

### 2.1 CubeSat state of the art

Ever since 1957, with the successful launch of Sputnik-1, thousands of satellites have been sent into space. They have had several tasks and purposes, ranging from scientific research to military uses. However, all these satellites shared some aspects in common: they all had a considerable big size and their investing cost was huge, so they were only affordable for billion-dollar revenue corporations, governments or military agencies.

Recently though, as technologies progress, the size of satellites has been greatly reduced, leading to the development of small satellites. These kind of satellites are characterised by their noticeable low wet mass (<500kg) and their relatively low investing cost compared to previous traditional satellites[19].

Smallsats	Wet Mass
Pico-Satellite	$\leq 1$ kg
Nano-Satellite	1 – 10 kg
Micro-Satellite	11 – 100 kg
Mini-Satellite	101 – 500 kg

**Figure 2.1:** Small satellites classification [1]

The introduction of really small satellites opened new market sectors which were previously unreachable for bigger and more expensive satellites. Medium-budget companies, public institutions or even private individuals can now launch their own satellite for a relatively moderate price. One outstanding example are the emerging satellite platforms known as CubeSats. Those nanosatellites, made up of Units of 10 cm edge cubes, are becoming a new trend that is spreading all around the globe.

Model	Mass [Kg]	Volume [cm <sup>3</sup> ]	SP power [W]	Battery capacity [Wh]
1U	1.33	1000	10	19.24
3U	4	3000	26	38.5
6U	8	6000	40	77

**Figure 2.2:** Physical and power typical constraints for <10kg CubeSats [2]

In fact, statistical data show that during the recent years the number of CubeSats launched into space has increased exponentially[3]. The number of launches has incremented so much

that it is even being called as a revolution, called as *New Space* revolution[20]:

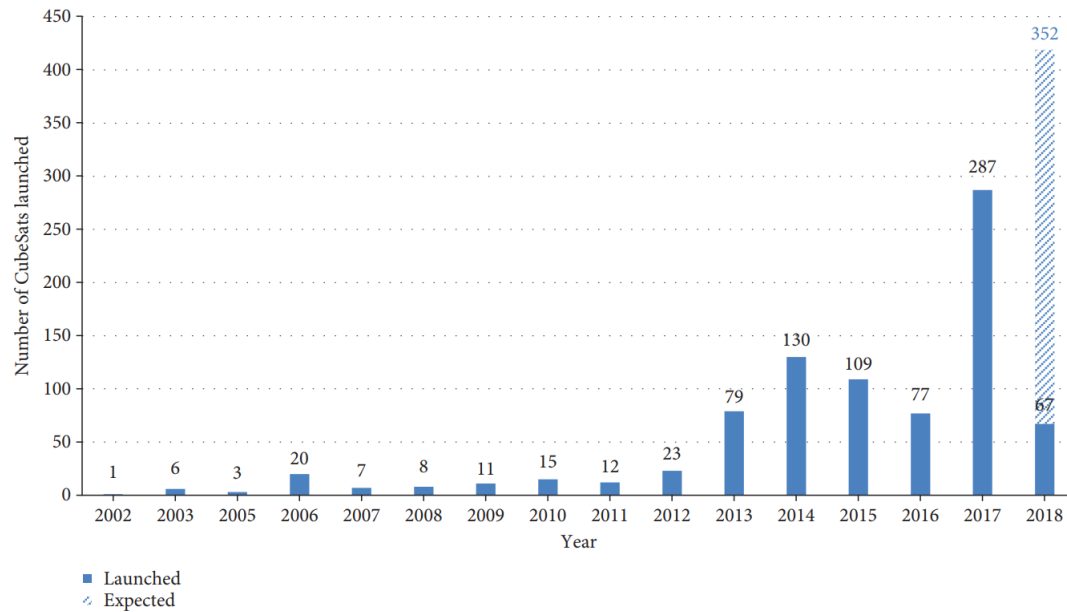


**Figure 2.3:** Evolution of launched CubeSats over years[3]

The huge reduction in manufacturing costs that has led into the astounding success of the CubeSat platform is principally due to two factors. Firstly, the miniaturization and simplification of all the satellite systems and subsystems. Secondly, the advances in Commercial-off-the-shelf (COTS) technology [21]. These components are low cost, low power, commercially available compact elements. Instead of the classic custom-made expensive space-graded equipment, COTS can be openly bought.

It is certainly true that the simplification of the satellites decreases their overall performance, but the reduction in costs allows for the manufacture of more satellites. This way, small satellites usually are part of a bigger flying formation or even an entire constellation of satellites.

Generally, such small satellites are used for applications such as telecommunications or EO missions and they are usually placed in Low Earth Orbits (LEOs), which range from an altitude of 120 to 2000km[22]. Low orbits offer some substantial benefits but they have important drawbacks too[23].

On one hand, they are closer to the Earth's surface. Therefore, in the case of EO missions, satellites can get images of the same quality than satellites in higher orbits even though the resolution required for any optical payload is lower. Placing a satellite in a low orbit is also more geo-spatially accurate, as attitude uncertainties do not propagate as much as in missions in higher orbits[4].

On the other hand, however, low orbits have some major inconveniences compared to higher orbits. Being closer to the Earth's surface also means that there are still some remains of the atmosphere left. The density of this residual atmosphere, while clearly is not as high as in sea level, strongly depends on Solar activity. The more solar activity, the wider the residual atmosphere and higher the density for the same altitude. The presence of atmosphere, even in cycles of low solar activity, generates atmospheric drag that slows down the satellites, making them leave their respective orbit and re-entering into Earth. Furthermore, the residual atmosphere is primarily composed of Atomic Oxygen (AO) particles, which are also highly reactive and corrosive.

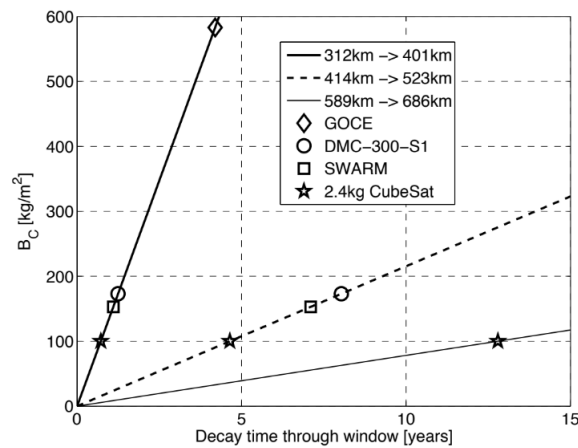


Figure 2.4: Decay time in orbit for various ballistic coefficients[4]

## 2.2 Micro-propulsion systems state of the art

Satellites in Very Low Earth Orbits decay in just a few days after being placed in orbit and the Spacecraft's Active Lifetime (SAL) is reduced drastically. This is the reason why satellites in such orbits required Corrective Propulsion Plants (CPP) as drag compensating measures to increase mission lifetime. Currently, many satellites in LEOs have got some sort of propulsion systems that activate when the satellites lose too much altitude. By expelling any kind of fuel, these conventional propulsion systems allow the satellites to recover altitude in order to return to the desirable orbit [5].

There are several types of micro-propulsion systems for small satellites [24][25]:

- Cold gas thrusters (CGT). They basically produce thrust by expelling a gas (usually nitrogen, helium or butane) contained in a pressurized tank. It is the simplest propulsion system and requires really low electric power. However, its specific impulse and fuel efficiency is really low, so its fuel consumption is elevate.
- Resistojet thrusters: with an operating principle similar to CGT, resistojets heat the propellant via an electrical resistance, at the cost of a really high power consumption. The fuel efficiency is improved.
- Chemical thrusters: chemical engine take profit of the combustion of a mixture of propellants (usually consisting of fuel and oxidizer ) to provide thrust.
- Electrostatic /electromagnetic thruster: Electric propulsion systems provide thrust by accelerating ionized propellant to high velocities. There are several kinds of electric propulsion systems, each one with a different method to ionize and accelerate particles. This thrusters have the highest specific impulse and therefore the lowest fuel consumption rate. However, they generally have low thrust-to-power ratio.



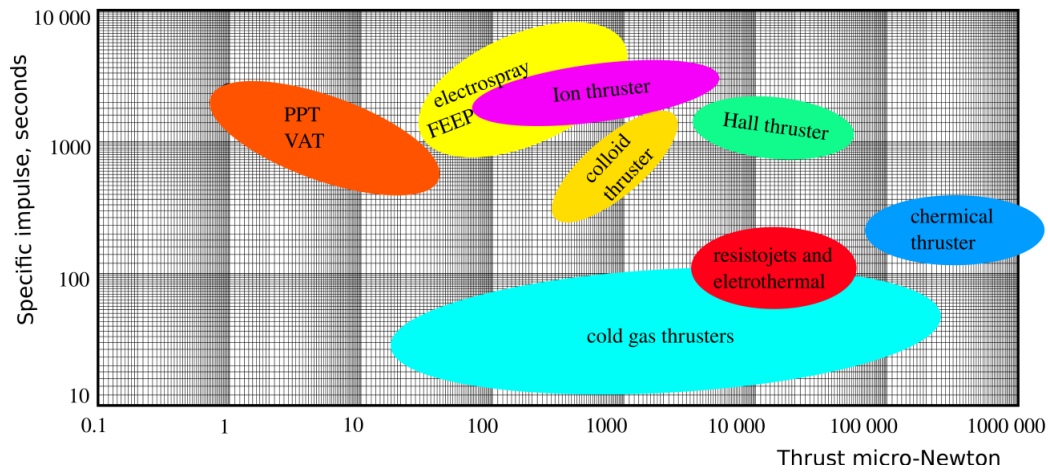


Figure 2.5: Characteristics of current conventional micro-propulsion systems [5]

## 2.3 ABEP and micro-ABEP state of the art

The problem is that the fuel used by these propulsion systems has to be carried inside the satellites. However, each extra kilogram of mass considerably increases the cost of launching the satellite. Therefore, small satellites do not carry large amounts of fuel, so, as soon as the stored propellant had run out, the propulsion system stops working and the satellites re-enter. With the considerable drag force effects in VLEO conditions, the fuel consumption by the CPPs can be huge and the amount of fuel that needs to be stored to sustain the satellite in orbit for a significant lifetime can be prohibitive.

This is why Air-Breathing Electric Propulsion (ABEP) systems are being developed. The ABEP concept, also known as atmosphere-breathing electric propulsion or ram-electric propulsion, was created to overcome such problem, enabling longer mission lifetime and reducing propellant mass requirement. The main idea behind ABEP systems is to provide thrust by utilizing the residual atmosphere at VLEO as propellant so fuel is no longer carried on-board. Therefore, the satellite fuel consumption will drastically decrease and at the same time the lifetime of the satellite will noticeably increase, hence increasing the overall profit generated by a single satellite[26]. Besides, eliminating the propellant mass also reduces the overall launch mass, significantly decreasing the launch costs of the spacecraft. Figure 2.6 illustrates the basic ABEP operating principle:

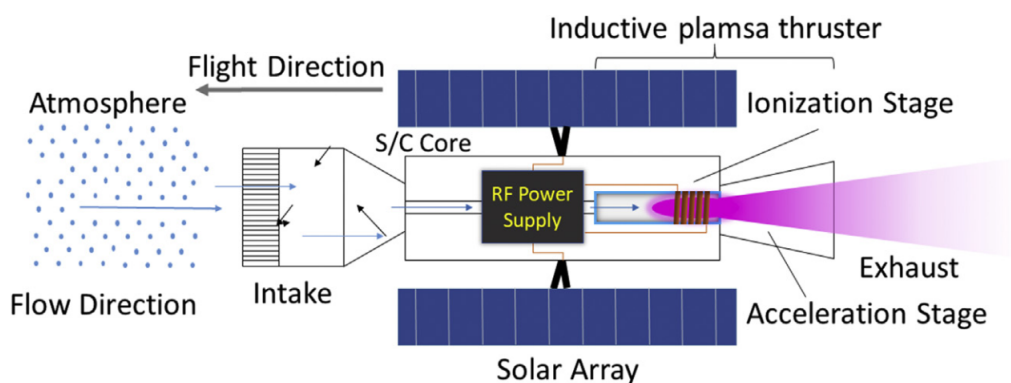


Figure 2.6: ABEP concept [6]

Nonetheless, ABEP technologies are currently under research and development, and it is still unclear whether or not they will be a more feasible propulsion system than traditional ones used in small satellites. They are far from totally researched or tested. In fact, many of the

ABEP projects have a low technological readiness level. Moreover, most of them are still in a preliminary phase of design.

Therefore it is difficult to find fully assessed ABEP engines and many of their parameters. Some of them, which are exposed in this bachelor's thesis, are just an estimation of the expected performance.

This is the principal target of this bachelor's thesis, to estimate if current ABEP systems could be a competitive means of propulsion systems used in satellites in EO missions at VLEO.

In order to become feasible, ABEP technologies have to deal with several challenges. They need to be capable of efficiently using the peculiar atmospheric species as propellant. But also of operating with really low mass flow rates and preferably, with low available power. Properly ionizing the residual atmosphere into useful propellant and while avoiding atomic oxygen electrode erosion are crucial design factors of the overall system [7].

ABEP missions are only feasible in a specific range of altitudes. The lower the altitude the higher the density of the atmosphere, so propellant mass flow rate is higher. However, this implies that the drag force is greater, so more power is required to fully drag compensation. On the other hand, at higher altitudes the mass flow rate can be so low that the engine may not be capable of collecting enough propellant mass flow for adequate operation [27]. Over 400 km, the influence of the drag perturbations over the lifetime of the spacecraft are quite slight, so conventional CCPs are clearly preferable rather than ABEP. For lower orbits though, the atmospheric drag forces becomes the strongest perturbation force, severely limiting the lifetime of satellite missions[7].

For satellites orbiting between 250 and 400km, the atmospheric gases could *theoretically* replace the entirety of the on-board propellant. In this situation, the mission profile in terms of lifetime will remain the same, but the mass that would instead be allocated as propellant can now be used for extra commercial/scientific payload. Otherwise, an ABEP system could complement another sort of CPP, further increasing the satellite lifetime.

For orbits in between 160 to 250 km, ABEP systems alone can totally compensate the drag perturbations and could maintain the spacecraft in orbit for an unlimited amount of time.

For orbits <160 km, neither the current ABEP systems nor the being developed ones can provide enough thrust to totally compensate drag, though they can elongate the satellite lifetime for some weeks.

However, according to the Jet Propulsion Laboratory (JPL), a minimum altitude has been established at 120km, due to heating effects. Actually, it is at 120km that it is considered that re-entry is [28]. Moreover, the power that ABEP systems would require for sustained operation at such low altitudes would be prohibitive.

This results agree with an ESA study conducted in 2007, where it was considered that air breathing electric propulsion systems are only truly competitive in the range of 120km to 250km [29]. For missions over 250km the amount of propellant required for conventional CCP is so low and the possible propellant flow rate for air-breathing systems is so small that ABEP can not compete with regular EP.

For a full drag compensation, the mean thrust force needs to be at least equal to the mean drag force(see eq8.1 in section3.1.3). At orbit altitudes ranging from 120 km to 250km, the orbital speed in which particles ram the satellite is around 7.8 km/s. Theoretically, the exhaust ve-

locity of the thruster  $c_e$ , should be at least this value to counter the drag force. However, it has to be taken into account that only part of the incoming mass flow rate gathered in the intake will later be used in the propulsion system. This collection efficiency,  $\eta_c$  is a critical design factor in any ABEP system and might drastically affect its feasibility as it will increase the minimum exhaust velocity.  $\eta_c$  depends on the size and geometrical parameters and design of the intake, but also on its specular reflection of particles, thus decreasing as atomic oxygen degrades the collector. Generally, two different type of intake setups are being used currently: a funnel-type design and a bypass-type design. Each one has its particular advantages and disadvantages, but they are considered out of the scope of this bachelor's thesis:

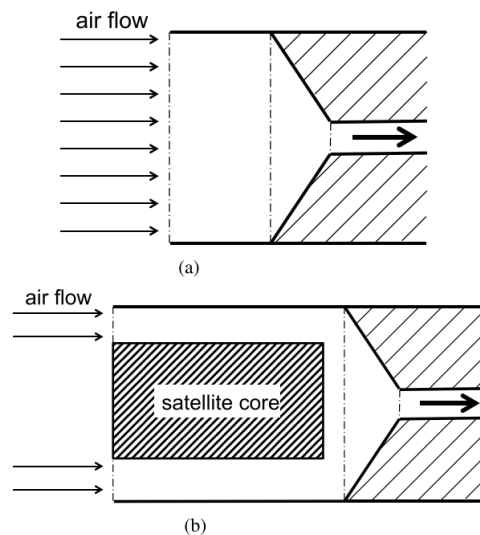


**Figure 2.7:** Intake Setups: (a) Funnel concept, (b) Bypass concept[7]

For an appropriate size of the intake and assuming compression factors of 100-200, collection efficiencies of  $\sim 40\%$  can be obtained[7].

### 2.3.1 ABEP designs review

In this section, some of the most relevant ABEP engines that have been designed or are undergoing a development phase will be reviewed.

Historically, the concept of ABEP systems is not new. In fact, the idea of replacing stored space fuel with the residual atmosphere gases originated back at the 1960s[7]. However, it was not until 2003 that real ABEP systems started to be developed[15]. Over the last 16 years, several ABEP designs have been developed and some have even been used in space mission, usually for technological demonstration.

Generally, ABEP systems can be classified according to the following scheme:

### 2.3.2 Air-Breathing Electrostatic Propulsion

AB electrostatic propulsion devices provide thrust based in the ionization, acceleration and neutralization of the particles (mostly  $N_2$  and  $O_2$ ) captured by the inlet.

The most common AB electrostatic propulsion systems are the air-breathing ion engines (ABIE) and the Hall Effect Thrusters (HET). These two have been the most researched ABEP designs.

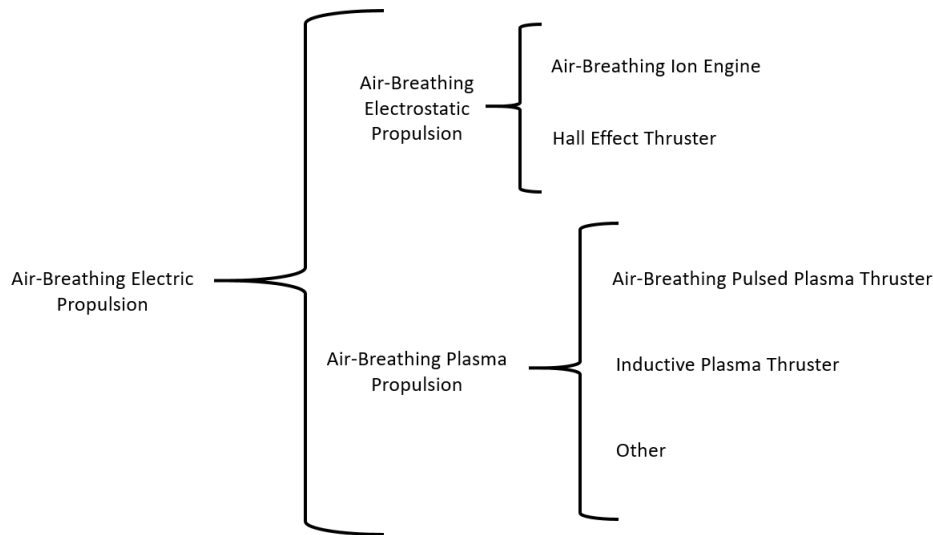


**Figure 2.8:** ABEP classification

The AB Ion Engine (ABIE) was the first ever ABEP system to be developed. It was designed to handle very low input pressures. The key elements of any ABIE system are: First of all, an air intake in which the propellant mass flow rate is collected. Followed by an ionization channel in which those particles are ionized and temporary stored, if needed. Finished by accelerator grids that will accelerate the outcome flow to the desired exhaust velocity so that drag is compensated. It is worth mentioning that a neutralizer would be added after the accelerator grids, so that the outcome flow is neutral and there is not an aggressive chemical degradation.

In fact, the only current example of ABEP system miniaturized for CubeSat applications is the ABIE thruster being developed by the University of Colorado, Boulder[15]. It is a low-weight, small-size ABEP system designed for 3U, 6U, 12U and 27U CubeSat Applications.

As an alternative to AB ion thrusters, Hall Effect Thrusters (HET) have higher thrust density, the ratio between thrust and the exhaust area. Henceforth, this allows a reduction of satellite cross-sectional area, thus reducing the overall generated drag.

However, preliminary studies show that both ABIE and HET systems have two major drawbacks. First of all, they require a high propellant flow rate that, depending on the collecting efficiency, might exceed the real possible mass intake for a certain altitude. Besides, for low mass flow rates, the engines will have a reduced thrust-to-power ratio. Furthermore, the flow of oxygen through the thruster can result in electrode erosion, which will severely limit the actual lifetime of the engine, becoming a substantial drawback[7].

### 2.3.3 Air-Breathing Plasma Propulsion

The AB plasma propulsion devices were developed in order to solve the electrode erosion constraint that AB electrostatic propulsion suffers from.

The solution was the development of Inductive Plasma Thrusters (IPT), which are electrodeless concepts, based in inductively heated plasma flows coming from Inductively Heated Plasma Generators (IPG). Due to the electrodeless design and the heated plasma flow, IPTs can operate using chemically aggressive propellants such as atomic oxygen without a significant reduction of the engine lifetime. Currently, IPT systems are being researched in the Institute of Space Systems (IRS) of the University of Stuttgart. They are developing and characterizing an IPG6.

Another example of plasma propulsion systems are the Air-Breathing Pulsed Plasma Thrusters (AB-PPT). They are still in a basic preliminary design phase, but it is expected that they will be able to efficiently operate with smaller mass intake and relatively low supply power: storage of the mass inflow will cut down the mass flow rate fluctuations, allowing further compression for a better thrust-to-power ratio, thus leading to a better performance. Furthermore, an inductively heated electrothermal plasma generator will allow the AB-PPT to handle hazardous gaseous mixture without negative side effects[7]. One advantage of the AB-PPT over the IPT is that the discharge frequency of the AB-PPT permits the system to easily regulate the power level according to the requirements of each pertinent orbit, thus considerably increasing the thruster lifetime.

So far, the project performance has not been tested in a proper test bench, so no experimental values exist.

## 2.4 ABEP lifetime expectancy

As mentioned, the ABEP technologies are still undergoing research and development. Many of them are still in preliminary design. In fact, even test facilities for ABEP systems are still being developed, so they are still far away from being normalized. Therefore accurate experimental data regarding ABEP performance is unquestionably scarce. Moreover, if it is taken into account that the tests conducted have only been undertaken a small fraction of time, the only chance of estimating the ABEP lifetime is a well-educated guess.

An ESA-CFD feasibility study report carried out in 2007 stated that, according to performance predictions, an average ABEP system could be used for missions with a spacecraft active lifetime from 3 to 8 years[29].

However, later experimental test with air-breathing electrostatic engines revealed that the thruster degradation due to interaction with reactive species such as oxygen had a more detrimental effect than expected, reducing the performance of the engine and severely shortening its total lifetime to  $\sim 10000$  hours, depending on the quality of the material.

This is why AB plasma thrusters are being researched; in order to cope with the electrode erosion so to significantly increase the engine total lifetime. Nonetheless they are not ready well studied so its expected performance and lifetime are merely predictions[7].

## Chapter 3

# Earth Orbits and physical environment

### 3.1 Classification of Earth Orbits

In the Solar System, there are several kinds of orbits an object can follow, ranging from hyperbolic to elliptic. Nonetheless, most satellites in Earth's close space follow an elliptic orbit. Those orbits can be described by three main parameters.

First of all, a satellite in an elliptic orbit around the Earth will be at a distance from the Earth surface, or altitude. The closer to the Earth's surface a satellite is, the higher its orbital speed. Therefore, satellites at low altitude will take less time to make a complete orbit around the Earth.

Another parameter is the eccentricity of the orbit. Eccentricity indicates how deviated the shape of an orbit is in comparison to a circle. Orbits with no eccentricity become circular, orbits with an eccentricity in between 0 and 1 (none of them included) are considered elliptic, orbits with an eccentricity of 1 are parabolic and orbits with an eccentricity higher than 1 are hyperbolic:

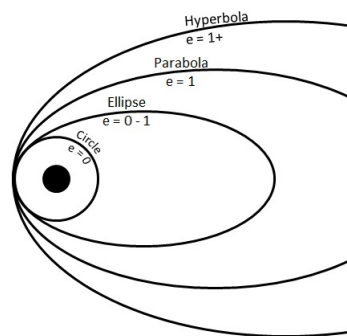


**Figure 3.1:** Orbit Eccentricity[8]

The last parameter to basically identify an orbit is inclination. The inclination of an orbit refers to the angle between the orbit plane and the Earth's equator plane, starting at 0 degrees when the orbit is directly above the equator:

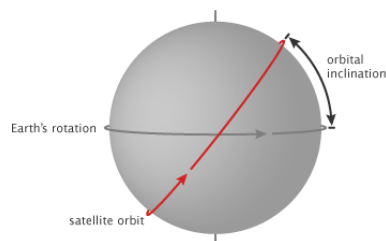


Figure 3.2: Orbit Inclination[9]

According to the altitude of the orbit and considering them as nearly circular (eccentricity close to or 0), orbits can be classified in three essential types of Earth Satellite Orbits: High Earth Orbit, Medium Earth Orbit, and Low Earth Orbit. Each one with its particular advantages and disadvantages[9]:



[9]

Figure 3.3: Types of orbits according to altitude

### 3.1.1 High Earth Orbits

Starting at 35780 km above the Earth's surface, High Earth Orbits or HEO are the most distant satellite orbits. At exactly 35780 km, satellites take around 24 hours to orbit the Earth. It is a remarkable fact as this to say that a satellite's orbital speed matches the Earth's rotation. Therefore, a satellite orbiting at an altitude of 35780 km will remain in place over the same longitude, though it might drift north to south and vice versa. This very special orbit is called geosynchronous. Besides, if a circular geosynchronous orbit plane matches the equator plane (inclination and eccentricity 0) it will become a geostationary orbit. A satellite in geostationary orbit will not have relative movement to the ground, so it will always be over the same place on the Earth's surface. This is of vital importance to weather monitoring satellites, as they will constantly cover the same wide area. It is also valuable for telecommunications (phone, internet, radio, television) satellites.

### 3.1.2 Medium Earth Orbits

Ranging from 2000 km to 35780 km altitude, Medium Earth Orbits or MEO are particularly suitable for Global Navigation Satellite Systems (GNSS) and telecommunications satellites. It is in this type of orbits that can be found remarkable satellite constellations such as the *U.S. Global Positioning System* (GPS), the European *Galileo* satellites or the Russian *GLONASS*. There are two remarkable medium Earth orbits:

- **Semi-synchronous Orbit.** It is a nearly circular orbit at 20200 km above the Earth's surface. Satellites in this orbit take approximately 12 hours to complete an entire orbit.

Therefore, satellites pass over the same spot on the equator twice a day, resulting in a highly predictable orbit. The *GPS* constellation orbits here.

- **Molniya Orbit.** This orbit has an inclination of 63.4 degrees and an eccentricity of 0.72. This highly elliptical orbit is used by the Russian space agency, *Roscosmos*, to deploy the GLONASS satellite constellation as it is quite useful for observing high latitudes:

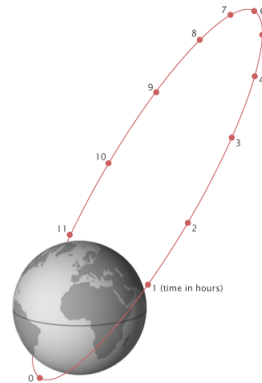


Figure 3.4: Molniya Orbit[9]

### 3.1.3 Low Earth Orbits

Starting at barely 120 km of altitude and extending up to 2000 km, Low Earth Orbits or LEO are the closest ones to the Earth's surface. While this type of orbit has not been as exploited as much the other two (specially the geosynchronous case), it turned out to have its own advantages and disadvantages. In fact, it is only in the Low Earth Orbit or Very Low Earth Orbit (VLEO, from 120 km to 450 km)[4] circumstances that Air-Breathing Electric Propulsion systems are indeed viable. Henceforth, it is worth explaining a how the LEO environment is like.

Amongst all the LEO orbits, it is worth highlighting the sun-synchronous orbit. These are orbits with an altitude in between 200 to 1680 km and a high inclination in which the sun lightning along the ground track remains almost constant over time, so the surface is always illuminated by the Sun at the same angle when viewed from the satellite. They are frequently used for Earth observation, solar study, weather forecasting and reconnaissance as there are not significant changes in shadows and lighting over time[10]:



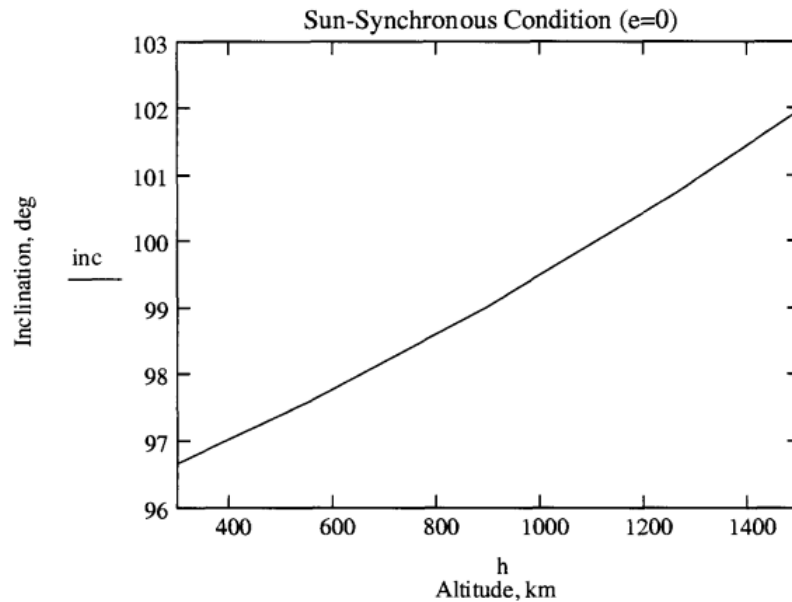


**Figure 3.5:** Sun-synchronous circular orbits as function of altitude [10]

Low Earth Orbit has a peculiar difference from either the MEOs or the HEOs, as there is still a presence of a residual atmosphere that has proven to be rather significant. The composition and density of this residual atmosphere is primarily driven by the Solar Extreme Ultraviolet (EUV) flux. The solar activity can be measured with the 10.7cm solar radio flux indicator (or  $F_{10.7}$ ), which indicates the output of the EUV radiation of 10.7 cm wavelength in units of  $10^{-22} \text{W/m}^2 \cdot \text{Hz}$ . The atmosphere also depends on the geomagnetic heating of Earth -designated by the  $A_p$  index- but in a much lesser extent [13]. Table 3.1 shows the maximum, mean and minimum solar and geomagnetic activity of the last 11-year solar cycle.

	Maximum	Average	Minimum
$F_{10.7}$	250	140	65
$A_p$	45	15	0

**Table 3.1:** Maximum, average and minimum solar and geomagnetic activity levels of the 2005-2016 solar cycle

Even though the solar activity cycle restarts once every 11 years, its  $F_{10.7}$  values never repeat themselves in the exact same way:

The most frequent elements that constitute the residual atmosphere are dinitrogen  $N_2$  and atomic oxygen  $AO$ , unlike the diatomic oxygen  $O_2$  that makes up for the primary element for the atmosphere at sea level. Atomic oxygen is formed at the LEO environment when diatomic oxygen gets photo dissociated by short wavelength solar radiation ( $<243 \text{ nm}$ )[12]. Figure 3.7 represents the average partial density of the most abundant species at LEO for mean solar activity:

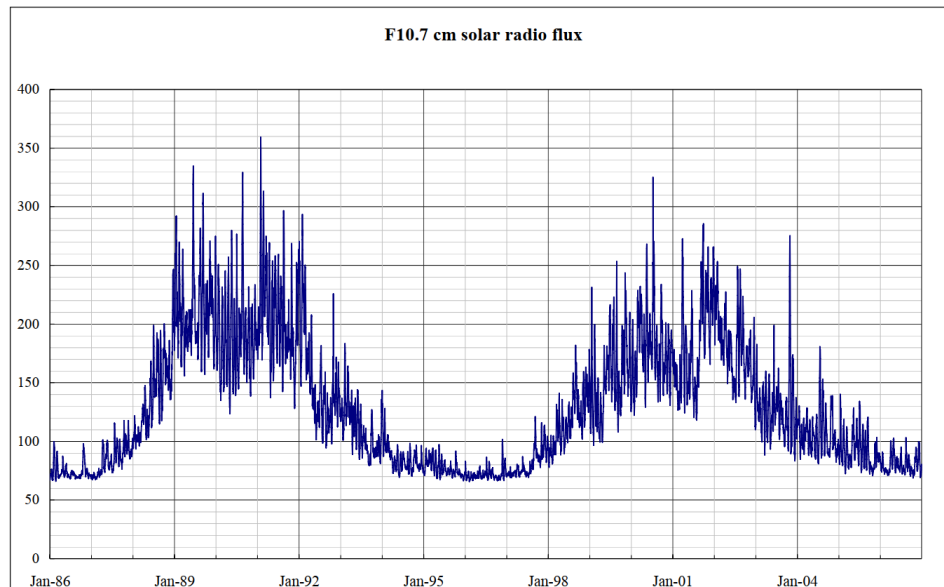


Figure 3.6: Solar activity over time [11]

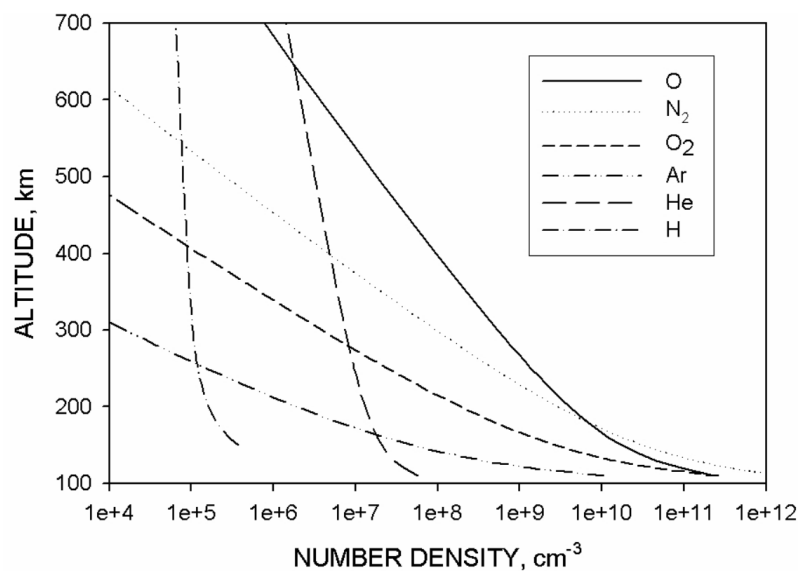
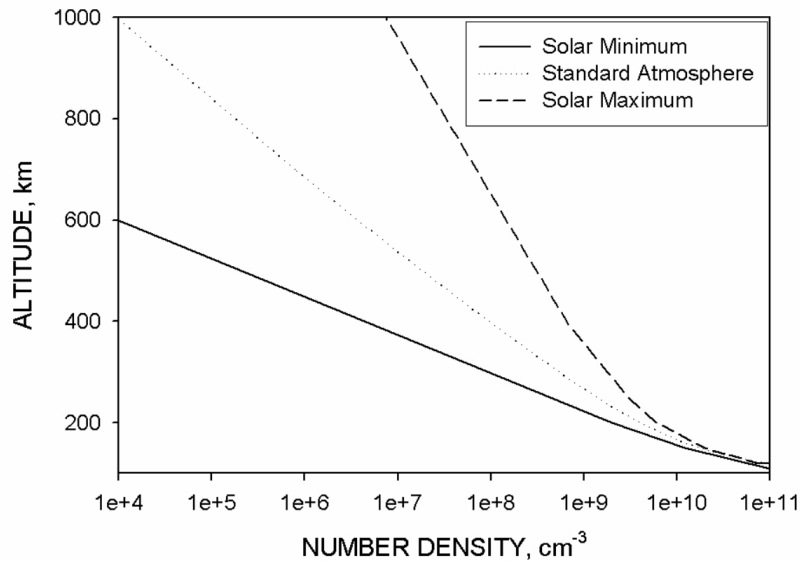


Figure 3.7: Partial density of atmospheric species as a function of altitude[12]

Nonetheless, the actual density of the several species not only depends on the altitude, but also on the level of solar activity. The more active is the sun, the more ultraviolet radiation gets to Earth, thus giving extra energy to the atmosphere, so that the lower layers rise and are replaced for even lower layers with higher density. This effect can be neglected at higher orbits but it is of great importance at LEOs[13]:



**Figure 3.8:** Average density of atomic oxygen as a function of altitude for minimum, nominal and maximum solar conditions[12]

The presence of atomic oxygen is a huge problem for spacecraft at LEO as it is much more reactive than diatomic oxygen[30]. As spacecraft orbit the Earth, they run into atomic oxygen at speeds of the order of 7.7 km/sec. This is when atomic oxygen can react with carbon surfaces, many metals and specially polymers. The continued exposure to atomic oxygen can lead to several sorts of damage, ranging from degradation of solar arrays or optic instruments; to the formation of cracks which can endanger the thermal control or even the whole structure of the spacecraft [12]. Overall, the atomic oxygen interaction poses a serious threat to the durability of satellites in LEO.

The interaction of materials with atomic oxygen is not the only inconvenience caused by the residual atmosphere. Although the air density is much lower than at sea level, the air resistance in LEO is still relevant enough to produce drag and pull the satellites down to Earth. In fact, till  $\sim 500$  km above the Earth's surface, the drag force is the major perturbing element on satellites (excluding the Earth's gravitational field)[13]:

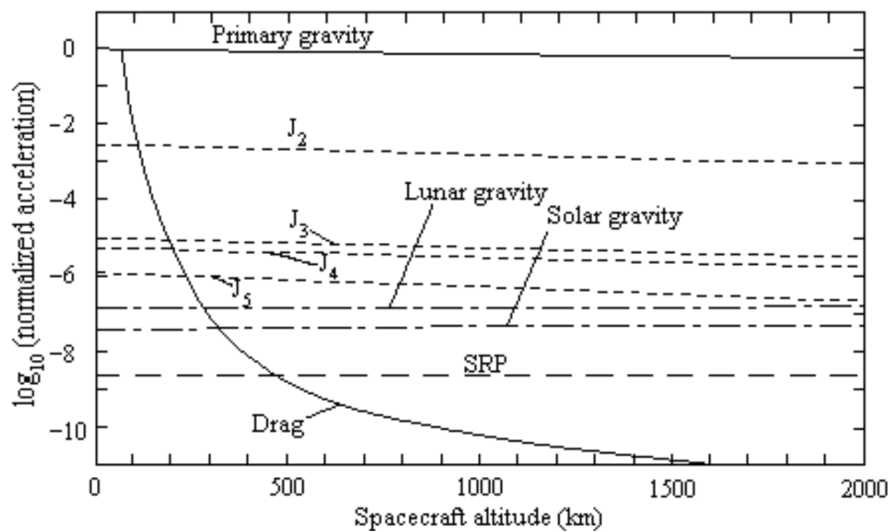


**Figure 3.9:** Comparison of different disturbing acceleration in LEO as function of altitude[4]

The drag force can be expressed by the relation:

$$F_D = \frac{1}{2} A \rho C_D V^2 \quad (3.1)$$

Where  $V$  is the velocity of the satellite -relative to the atmosphere and assuming that the satellite's absolute speed is aligned with the absolute speed of the atmospheric particles-,  $A$  is the vehicle cross-sectional area,  $\rho$  is the total density of the atmosphere and  $C_D$  is a dimensionless drag coefficient.  $C_D$  depends on the altitude, surface deterioration (due to atomic oxygen interactions) and shape of the satellite, varying from 2.1 to 2.7. Generally, for conventional shaped satellites orbiting at very low earth orbit, a value of 2.2 is assumed[7]. Equation 3.1 can also be expressed as:

$$F_D = \frac{1}{2} \frac{m}{B_C} \rho V^2 \quad (3.2)$$

Where  $B_C$  is the ballistic coefficient, known as the total spacecraft mass  $m$  divided by the vehicle cross-sectional area and drag coefficient. Figure 3.10 represents the drag force as a function of altitude for usual satellite cross-sectional areas and in mean solar activity conditions:

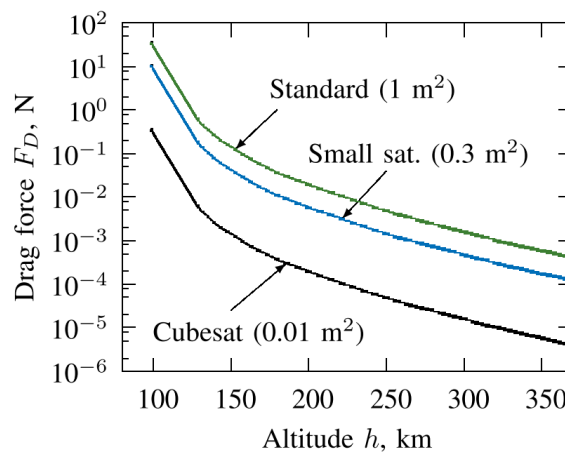


**Figure 3.10:** Drag force as a function of altitude for different cross-sectional areas and in mean solar activity conditions[7]

As mentioned, the density depends on the altitude and the solar activity. Therefore, the drag force perturbation effects are also related with the ultraviolet radiation variations. Figure 3.11 shows the semi major axis and eccentricity perturbations that the drag force exerted on the PRIRODA module satellite, at around 385 km of altitude; for minimum and maximum solar activity:

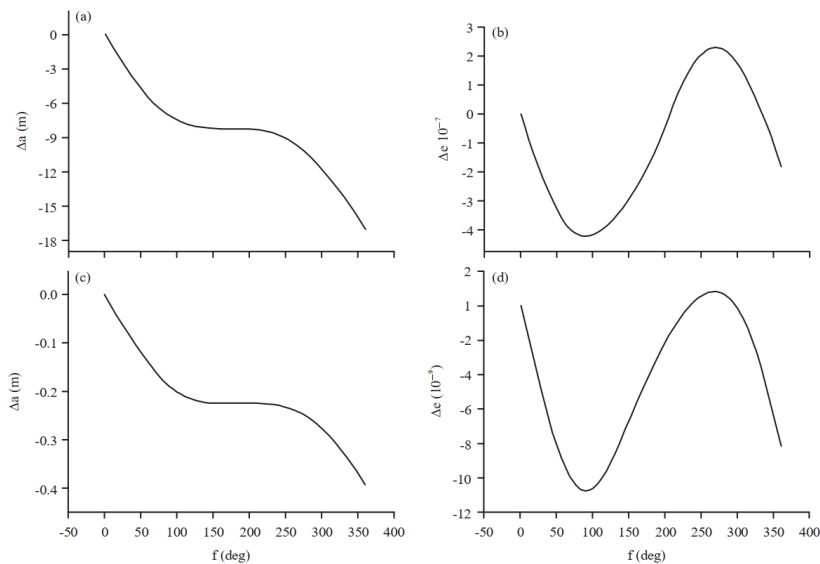


**Figure 3.11:** Variations of semi major axis and eccentricity as function of true anomaly during maximum solar activity (a-b) and minimum solar activity (c-d) for PRIRODA satellite[13]

Therefore, even with minimum solar activity, drag experienced by the satellites orbiting at LEO is a perturbation force that must be considered to expand their time in orbit. This is the reason why many satellites carry some kind of propulsion device to keep them in orbit. Furthermore, the ABEP technologies are being developed to profit from the residual atmosphere so that less amount of fuel or even no fuel is carried inside the satellite, while enhancing its lifespan in orbit.

An other important term of the LEO environment is the ionizing radiation. The radiation in Low Earth Orbit is essentially a mixture of Galactic Cosmic Rays (GCR), charged particles trapped in the Van Allen belts and Solar Energetic Particles (SEP). GCR originate from outside our solar system and contain particles of all charges, from protons to even uranium nuclei. The flux of GCR is inversely proportional to the solar activity, being the lowest while the solar activity is at its maximum. The Van Allen Belts radiation belts are zones that encircle the Earth where charged particles such as protons or electrons are trapped by the Earth's geomagnetic field. Finally, Solar Energetic Particles come directly from the Sun and have different energy, depending on the type of particle or the activity of the 11 year solar cycle[31]. Generally, the ionizing radiation can cause single-event upsets in electronic circuits and create noise in sensitive instruments[30].

Finally, one last aspect that has to be contemplated in the LEO environment is the presence of meteoroids and man-made debris. Over the last decades, space debris has risen dramatically and has become a serious issue to take into consideration. The most common objects left in these orbits are wastes resulted from orbital-transfer rocket stages that group together to form a debris cloud, orbiting at velocities as high as 90 km/s. A single hyper-velocity impact can cause severe structural damage and generate punctures, fractures or cracks which can further expose the underlying material to atomic oxygen interaction or ionizing radiation, leading to a catastrophic failure of the mission[30].

### 3.1.3.1 Atmosphere model

Now that the LEO environment characteristics have briefly been reviewed, it is time to explain how the atmosphere conditions can be modeled.

Nowadays, modelling techniques of the atmosphere conditions (temperature, total density, partial density, conductivity, etc.) are based on empirical data retrieved by satellites and atmospheric probes ever since the 1960s. In 1976, the International Standard Atmosphere (ISA) was the first standard to model the atmosphere as a function of altitude. Later on, with increased atmospheric data collected from space, the NASA Goddard Space Flight Center came up with the Mass Spectrometer and Incoherent Scatter (MSIS) model, which included the composition of the residual atmosphere and the partial densities of its species. Over the years, this model was expanded and corrected till the current Extended MSISE-90. Moreover, the Naval Research Laboratory made further improvements to the NASA MSISE, resulting in the NRLMSISE-00 model, which takes into account the presence of anomalous species in the atmosphere.

Another parallel model is the Jacchia-Bowman (JB) model, created in 2006. It has an improved representation of thermospheric absolute density variations, but it does not predict the residual atmospheric composition nor the partial densities of the several atmospheric species.

Both MSIS and JB models are refined constantly and can be found summarized in the European Cooperation for Space Standardization (ECSS) standard ECSS-E-ST-10-04C issued in 2008.[11].

## Chapter 4

# Benefits and Challenges of orbiting in Low Earth Orbit

Now that the Low Earth Orbit has already been described, it is time to analyze the peculiar advantages and disadvantages that might have satellites which orbit in them. As stated in the scope of this project, the main satellites that are going to be reviewed are the ones related with Earth Observation missions.

### 4.1 Benefits and advantages

LEO type of orbits are the closest ones to the Earth's surface. Flying closer to the observation target or, in other words, reducing the operational altitude can allow the performance of the LEO satellites to match with those of the satellites in higher orbits but with simpler and smaller platforms, thus lowering the cost of the mission. The most relevant benefits of operating in LEO are[4]:

- Improved resolution of optical payloads. The maximum theoretical resolution of an optical system can be determined using Eq. 4.1:

$$r = 6.71 \times 10^{-9} \frac{h}{D} \quad (4.1)$$

Where  $r$  is the ground resolution,  $D$  is the aperture diameter and  $h$  is the satellite altitude. Therefore by reducing the operating altitude, the ground resolution is increased without even modifying the quality of the optics.

- Increased radiometric performance. As the distance between the satellite and the target becomes lower, there are less possible interference that might get in the way of the instruments. This is to say that the ration between signal to noise is higher, furthermore allowing for a cheaper less sensitive radiometer to achieve the same results as the more expensive ones used in higher orbits. Besides, the antennas' gain is lower so they require less power.
- No de-orbit method required. In 2015, the European Space Agency, following the Inter-Agency Space Debris Coordination committee (IADC) recommendations, stated that all new inactive spacecraft should re-enter within 25 years[32]. Nonetheless, thanks to the drag force effects, all satellites in LEO left without an active propulsion system will de-orbit in less than 5 years.
- Increased geospatial position accuracy. A shorter path length to the target involve smaller arm length for uncertainties to propagate. Therefore, EO images taken by the satellite can be geolocated more accurately.

- Low revisit timeliness. Satellites in Low Earth Orbits have the highest orbital speeds. Hence, the periods of time in between flying over the same ground spots are shorter than satellites in higher orbits.
- Reduced latency. The lower altitude of LEO satellites mean that the data trip between the satellite and the ground is reduced, thus significantly improving the latency.
- Cheaper launches. As a general rule, the higher the orbit required for the satellite, the more expensive launches become. Therefore using VLEO can certainly reduce the investing money required to place a CubeSat in orbit which, actually, is one of the biggest expenditures of the satellite imagery industry.

## 4.2 Challenges and disadvantages

On the other hand, orbiting at LEO has some important drawbacks compared to higher orbits, most of them due to the extreme LEO environment:

- Strong aerodynamic forces and torques. The presence of the residual atmosphere, as function of the altitude and the solar activity, generates an important drag force that, generally, is considered as an unwanted effect that needs to be compensated using propulsion systems. Besides, the aerodynamic torques may also pose a challenge to attitude control systems.
- Atomic oxygen erosion. As mentioned in the previous chapter, AO is one of most abundant atmospheric species at LEO, being a highly reactive element that can degrade the sensor surfaces and damage the satellite surfaces.
- Short communication windows. The high orbital velocities also mean that the time apertures in which the satellite can transmit data to the ground station are considerably short. This is to say that the ability to downlink or uplink data to a same ground station is severely limited. Therefore satellites in LEO must have high data rates, leading to the use of higher bandwidth communications subsystem, increasing the cost.



# Chapter 5

## ABEP scenario proposal

In order to successfully accomplish the aim of this bachelor's thesis and therefore make an analysis of ABEP systems as nano-thrusters for EO CubeSat applications, an hypothetical scenario will be presented and upon it a feasibility study will be done.

The scenario will be that of a short term EO commercial mission at VLEO, which is likely to happen in the near future. Such mission is going to be carried out by a nano-satellite following the CubeSat Design Specifications (CDS) [17]. In this case, a nano-propulsion system will be incorporated as a single primary propulsion plant for full drag compensation.

A possible conceptual CubeSat design for EO commercial applications in VLEO will be presented, with two possible configurations. The first one will be a conventional propulsion system with an on-board stored fuel. The second time, an ABEP system will be set up.

For both configurations, a summarised mass and power budget of the different CubeSat elements and systems, based on COTS products, will be conducted. Furthermore, a brief manufacturing cost budget for each layout will be done. Afterwards, the operating viability of each propulsion system regarding mass and power restrictions will be evaluated. Finally, considering the mass and power limitations of each propulsion system, a feasibility study for ABEP systems as nano-thrusters will be carried out.

### 5.1 Scenario parameters

In this section, the scenario parameters and the decisions that were taken to realize this study -concerning the EO mission, CubeSat conception, the conventional propulsion power plant choice decision and the ABEP system choice- are explained. In addition, the assumptions adopted in the study are disclosed.

#### 5.1.1 Orbit proposal

Due to the fact that the study will be based on a commercial EO CubeSat, a sun-synchronous circular orbit has been picked, as it offers beneficial conditions to EO missions (see Section 3.1.3). The orbit altitude in will be varied among the VLEO range (160-450 km). However, for a preliminary orbit design an altitude of 250 km will be set as initial consideration.

Under Newton's law of universal gravitation, the orbital period of any circular orbit can be obtained by:

$$T = \sqrt{\frac{4\pi^2(R + r)^3}{\mu}} \quad (5.1)$$

Where  $T(s)$  is the orbital period,  $R(m)$  is the celestial body radius,  $r(m)$  is the orbit altitude and  $\mu(3.986e14 \text{ m}^3/\text{s}^2)$  is the standard gravitational parameter of the celestial body, calculated as the Earth body mass  $M(\text{kg})$  multiplied by the universal gravitational constant  $G(6.67428e-11 \text{ m}^2/\text{kg} \cdot \text{s}^2)$ :

$$\mu = G * M \quad (5.2)$$

In the case of a circular Earth orbit at 250km of altitude, the resulting orbital period is of 89.36min, leading to 16.11 orbits/day. From the total orbit period, it is conservatively to assume that 40% of it will be in eclipse [33]. During those 35.74 min the solar arrays will generate no power, so the electric batteries will have to deliver it. As for total lifetime in orbit, a modest 1.5 year mission duration will be considered.

Additionally, the orbital speed  $V_o(m/s)$  can also be calculated using the law of universal gravitation:

$$V_o = \sqrt{\frac{\mu}{R + r}} \quad (5.3)$$

Where  $R$  is the Earth's radius and  $r$  is the orbit altitude.

Table 5.1 includes the orbit's main parameters:

Orbit type	Sun-synchronous Earth orbit
Altitude	250 km
Eccentricity	0 (circular)
Inclination*	$\sim 95^\circ$
Orbital speed	7759.02 m/s
Orbits per day	16.11
Total orbital period	89.36 min
Sun-light time	53.61
Eclipse time	35.74 min

**Table 5.1:** Reference orbit for the CubeSat conceptual design

For orbit density prediction as a function of altitude, the JB-2006 model will be used [11]. As explained in Section 3.1.3, this model is specially useful to figure out the total density of the atmosphere over a certain altitude, which is needed to obtain the drag force (see Eq. 8.1).

### 5.1.2 CubeSat conception

The chosen spacecraft design has been that of a 6U (3Ux2U, dimensions  $\sim 30 \times 20 \times 10 \text{ cm}$ , 1.33 kg per Unit) EO CubeSat carrying an optical camera as single payload, similar to many EO CubeSats that some satellite imaging companies are employing currently [34]. The CubeSat size has been selected as 6U because smaller configurations imposed too strict mass and power constraints, whereas bigger ones meant extra satellite complexity, see Figure 2.2.

The optical payload was selected as its relatability with today's imaging industry allowed for a simpler income forecast model [35]. A single payload was adopted as the lower the mass and power spent in the payload subsystem, the higher the mass and power is available for the propulsion subsystem.

The CubeSat preliminary design will be done in compliance with the 13 Rev. CubeSat Design Specifications [17]. The already severe constraints of such a small spacecraft will need to be balance out so that it can hold a nano-propulsion system to perform in a possible VLEO commercial mission scenario. All of the CubeSat elements will come from a COTS origin when possible (see Section 2.1).

The CubeSat orientation towards earth is represented in Figure ??:

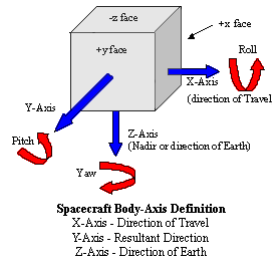


Figure 5.1: CubeSat orientation towards Earth

Where the x-face will be the 2Ux1U face and the z-face will be the 2Ux3U face. This way, the cross-sectional area will be minimum, thus reducing the total drag force.

### 5.1.3 Conventional propulsion power plant decision

Among all the the possible propulsion systems for CubeSats reviewed in Section 2.2, there is clearly just one option that might be suitable as a nano-propulsion thruster for an EO CubeSat mission: the electric thrusters, either electrostatic or electromagnetic [25]. Other propulsion systems such as cold/hot gas or liquid mono-propellant might provide higher thrust, but their low specific impulse will lead to a humongous fuel mass consumption, see Figure 2.5.

There are two categories of electrostatic thrusters: ion engines and hall effect thrusters. Even though both have rather similar performances, ion engines usually have higher specific impulse, leading to a lower propellant mass flow rate. Therefore, as the critical design factor for the conventionally thrusted CubeSat is probably going to be the available mass for propellant, an ion engine will be adopted in this study. Besides, ion engine also offer a highly controllable very precise steady thrust, thus leading to lesser disturbances and easier, more accurate pointing [36][33]. This is outstandingly suitable for formation flying or even constellations [36].

However, most nano-ion engine systems are yet under development, so they are still being tested used in experimental technology demonstration missions [5]. The only nano-thruster with a high enough technological readiness level that is currently at miniaturized CubeSat scale and available for commercial missions is the IFM nano-thruster engine developed by FOTEC and manufactured by the *Enpulsion* company.

It is a Field Emission Electric Propulsion (FEEP) system which generates thrust by accelerating ions via electric fields. The ions come from the propellant reservoir and are expelled at really high exhaust velocities:

The IFM thruster uses indium as solid propellant. It's incredibly high specific impulse allows for a really low fuel consumption. Its main drawback is the relatively low thrust-to-power ratio, which implies that the thruster requires a high amount of electric power supply and a complex Power Processing Unit (PPU) [37].

The characteristics of the IFM nano-thruster can be found at Table 6.14 in Section 6.2.6.

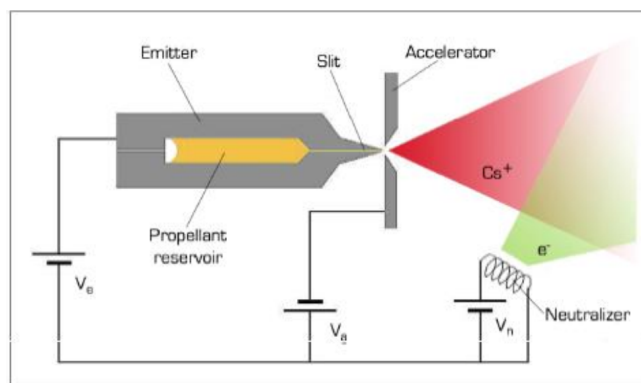


Figure 5.2: Schematic representation of FEEP operation [14]

#### 5.1.4 ABEP decision

As stated in Section 2.3, ABEP are still in early phases of development. Even more so, miniaturised ABEP systems capable to fit inside CubeSats are in really low stages of technological readiness. Nonetheless, the University of Colorado has developed a conceptual design of an ABEP thruster which would be able to work inside the small CubeSat frame [15]:

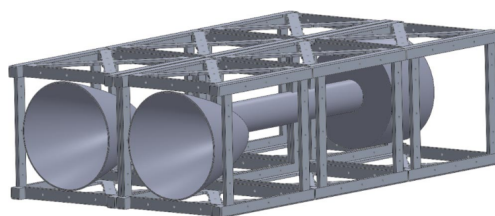


Figure 5.3: Mock-up of the 6U AB-GIE thruster system [15]

It is an Air-Breathing nano Gridded-Ion Engine (AB-GIE) which collects some of the species left in the residual atmosphere (mainly  $N_2$  and  $O_2$ ), ionizes them and accelerates them so that they exhaust at high velocities. It's inner workings are quite similar to the IFM thruster, but in this case there is not need for a fuel storage tank which makes for a great advantage over traditional propulsion units:

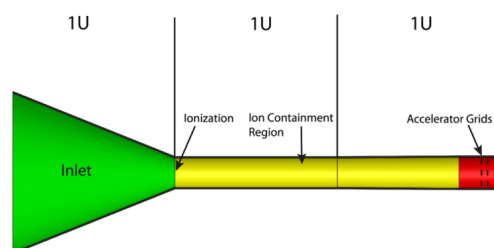


Figure 5.4: Schematic representation of ABEP operation [15]

Even though this design is still undergoing simulation, it is expected that the engine could provide relatively high thrust compared with other nano-propulsion systems. However, this ABEP system currently presents some major drawbacks. First of all, the inlet and ionization efficiencies are quite low, so the overall system itself has a low thrust-to-power ratio which means that it requires a lot of electric power consumption. Secondly, collecting atmospheric species at VLEO does unfortunately imply gathering AO. As mentioned in Section 3.1.3, such element is highly corrosive so a continued operation regime of the ABIE at VLEO would lead to a rapid deterioration of the propulsion system, highly reducing its operating lifespan.

Although the ABIE is still in early phases of development and testing, it's expected perfor-

mance characteristics can be found at Table 7.1 (see Section 7).

### 5.1.5 Adopted assumptions

It has to be taken into account that the purpose of this bachelor's thesis is not to provide an in-depth CubeSat design or to determine a meticulous mass and power budget of a CubeSat. Neither it is to implement an detailed value chain of CubeSat platforms nor to establish a rigorous income model for CubeSat satellites. Furthermore by the time of this project was conducted, many nano thruster technologies are still undergoing a phase of development and testing, specially concerning ABEP. Therefore, some assumptions were taken to simplify this study in order to keep it inside its scope. Furthermore, some values in this study may turn out not to be completely accurate. Moreover, as ABEP systems are more researched over time, some performance parameters are likely to significantly change.

The following statements and hypothesis have been embraced in this study, selected for several criteria:

1. As it will be a short-term EO mission, the variations of the solar cycle over time will not be considered.
2. Atmosphere changes due to orbit inclination will be neglected.
3. Atmosphere changes in the day-night cycle will not considered.
4. Earth oblateness and shadowing effects will not be considered.
5. AO insulation techniques will not be studied.
6. Degradation due to AO will only be accounted in the degradation of solar arrays. It will not be taken into account CubeSat structural degradation, changes in the CubeSat optical or thermal surfaces due to AO degradation. Nor changes in the thruster performance or efficiency.
7. No mechanical or structural analysis of the CubeSat will be done.
8. No satellite heat transfer analysis or thermal budget will be done.
9. No bus or link design will be done.
10. Satellite stability due to torques will not be analyzed.
11. Volume constraints will not studied. CubeSat internal volume element distribution not analyzed. The internal arrangement of components will not be disclosed.
12. It will be considered that the power-to-thrust ratio of the ABIE thruster will remain constant, independently of the altitude and solar activity.
13. The transitory interval in between launcher deployment and the stationary establishment will not be considered
14. The dimensionless drag coefficient  $C_D$  will be assumed as a canonical 2.2, used in the literature [7].
15. No redundancy design will be done in neither of the CubeSat configurations..
16. In order to minimize drag, the solar arrays surface normal vector will be perpendicular to the incident flux. Doing so implies that the solar radiation does not reach the solar array at an optimum angle [33]. In some specific cases, this drawback could drastically reduce the total supplied power generated by the photo-voltaic cells. Therefore,

many commercial satellites have auto-adjustable solar arrays that keep rearrange for the appropriate incidence angle. However, doing such thing in VLEO would imply a significant increase in drag as the cross-sectional area would increase too. In this study, the effects of solar incidence angle in the solar arrays will not be considered.

17. At VLEO range, the total density of the atmospheric species is so low that the stream of particles is not longer continuous, but rather each particle is seen individually. Such state is known as free molecular flow. Nonetheless, drag calculation in free molecular flow requires highly complex models. Therefore, for the simplicity of this study it will be considered that the particle flow impacting into the satellite will be continuous and homogeneous. Besides, it will be supposed that such flow does only come in the ram direction.
18. It will be assumed that the cross-sectional area will always remain the same.

## Chapter 6

# CubeSat design using the IFM nano-thruster approach

In this chapter, a conceptual design and sizing will be done for the 6U CubeSat carrying the IFM nano-thruster on behalf of a conventional propulsion system (see 5.1.3).

As with every satellite, the design of this CubeSat can be decomposed in 2 key segments: the structural architecture and the satellite systems and subsystems. In this particular case, that of a CubeSat employing a conventional propulsion system, the design will be primarily driven by the strictly limited available propellant mass. Besides, the small electric power supply in nanosatellites will also be a restricting factor (see Figure 2.2).

The preliminary description, sizing and arrangement of this aforementioned key elements is presented below:

### 6.1 Structural architecture

The structure will be the primary chassis of the CubeSat. It has to physically support all systems and subsystems while being able to resist to the mechanical loads that the satellite might experience during its lifetime, for example during the launch phase. It might as well provide thermal and radiation shielding for sensitive components on the inside. It usually consists of a hollow frame with interior braces and brackets serving as mounting points for the different components inside the CubeSat. The frames are generally made from aluminium as it is a low weight, low cost material with high specific strength. Additionally to the core frame, once the components are mounted inside the CubeSat, external metallic or fiberglass panels cover the satellite to shield the internal components and to provide mounting points for the solar array.

A 6U CubeSat structure, which follows the CubeSat Design Specifications, has been found online:

Element: 6U CubeSat structure	
Parameter	Value
Total mass	1100 g
Inside envelope	960x960x849 mm
Outside envelope	1000x2263x3405 mm
Thermal range	-40 to +80 °C
Manufacturer	ISIS
Price	7850€

Table 6.1: 6U CubeSat structure parameters

Both mass and price include the frame, the interior braces and brackets and the external metallic panels.

## 6.2 Systems and subsystems

Now that the structural architecture has been found, its time for the several systems and subsystems. Generally, there are 7 different satellite systems:

- Payload system.
- Attitude Determination and Control System (ADCS).
- Communication system.
- Command and Data Handling System.
- Propulsion system (not common in CubeSats).
- Thermal control system.
- Electrical power system.

### 6.2.1 Payload system

Even though the main target of this bachelor's thesis is the study the nano-propulsion systems in VLEO, the actual purpose of every CubeSat commercial missions is to generate value out of a hosted payload. This is why a single but yet competitive high quality payload has been included in this preliminary design. Nonetheless, its optical properties and performance will not be analyzed in depth.

The chosen payload has been a high resolution nadir-looking *Chameleon Imager*, configured as a high frame rate RGB Bayer-pattern panchromatic (PAN) camera:

Element: High framerate RGB Bayer-pattern camera	
Parameter	Value
Total mass	1350 g
Dimensions	200x94x94 mm
Power consumption (Readout mode/ imaging mode)	2.5 W / 3.5 W
Price	116000€
Manufacturer	SAC
Image resolution (Mp)	3.6
Spatial resolution (at 500km)	9.6 m
Swath (at 500km)	32 km

Table 6.2: *Chameleon Imager* panchromatic camera parameters



The last 3 parameters of Table 6.2 are optical properties of the payload itself. On one hand, the image resolution is the number of pixels captured in a single digital image, generally expressed in Megapixels (Mp). The amount of Megapixels per image and bit/pixel ratio dictates the size of the file. As this camera has a JPEG2000 frame data (with a typical compression ratio of 10:1) and a 8 bit/pixel ratio, each photograph of 3.2 MP will have a size of 0.32MB [38].

On the other hand, the spatial resolution or, more appropriately, the Ground Sample Distance (GSD) points out the ground distance equivalent to the distance of the center of two pixels in the image. This parameter is of vital importance as it dictates the selling prices of the outcome satellite images. Table 6.3 illustrates current commercial resolution types and their corresponding selling prices:

	Very high resolution	High resolution	Medium resolution	Low resolution
GSD (m)	0.3-1	1-5	5-10	>10
Custom requested imagery price (€/km <sup>2</sup> )	13.322	7.105	1.261	Free*
Archive imagery price (€/km <sup>2</sup> )	7.105	3.552	0.888	Free*

**Table 6.3:** Current imaging resolution parameters

Custom requested images refer to customer *ad hoc* specifically demanded images, while archive images refer to images that the satellite has already taken and that have been stored in its archive. The asterisk for low resolution imaging prices mean that any customer can get the image for free as long as self-accessed.

Regarding Table 6.3, it can be seen that the *Chameleon Imager* operating at 500 km would be included into the medium resolution range. Nonetheless, taking into account Eq. 4.1 from Section 4.1, it can be remarked that when the same payload operates at around  $\sim 260$  km its GSD goes down to 5m, which would be considered as High resolution, thus substantially increasing the selling imaging prices (specially for requested images).

Finally, the swath measures the portion of the Earth's surface that the camera payload is able to capture as the satellite orbit around the Earth. It can be calculated by:

$$Swath(km) = GSD(m) * Imageresolution(Mp) \quad (6.1)$$

Again, considering that the image resolution does not change, the swath of the *Chameleon Imager* operating at  $\sim 250$  km would be of 16 km.

Additionally, the payload has an integrated mass storage of 160 GB, so no extra payload storage will be needed. A big storage capability will allow the CubeSat to keep making images without overwriting them in the hypothetical case that the satellite could not establish communication with ground station. However, having such data storage would be pointless if the communication system is not able to transmit (to the ground station) the stored data at a sufficient downlink rate.

## 6.2.2 Attitude determination and control system

The purpose of the attitude determination and control system is double. Firstly, it has to measure the position of the satellite's orientation with respect the center of mass (attitude sensors). Then, in case the attitude has been disturbed, the ADCS has to rapidly correct it so that it is accurately maintained (attitude actuators). An appropriate attitude maintenance is essential for optimal communications, solar panel orientation and payload performance. Furthermore, in the case of satellites in VLEO it is also important to control the thrust direction and the satellite orientation towards the incoming air mass flow in order to minimize the

cross-sectional area of the spacecraft, thus reducing drag.

The attitude can be perturbed by several factors, the most important of them and their respective torques are listed below:

Disturbance	Torque (x10e-8 N·m)
Gravity gradient	9.0
Solar radiation pressure	3.1
Magnetic field	450
Aerodynamic	~4000

**Table 6.4:** Average disturbance torques acting on a 6U at 400km [16]

It should be mentioned that as the satellite has a thruster, torques due to the propulsion system should also be considered. However, for a simplified analysis, they are going to be neglected.

#### 6.2.2.1 Attitude sensors

The main task of the attitude sensors is to detect and diagnose the orientation of the CubeSat with regards to its center of mass. Most CubeSats utilize sun sensors, as they offer a considerably great accuracy (of about  $0.5^\circ$ , 3-sigma) at a cheap price. This is to say that for a satellite orbiting at 300km, a nadir payload would have a ground uncertainty of 2.6km:

$$\text{Grounduncertainty}(km) = \text{Tan}(\text{attitudedeterminationaccuracy}) * \text{orbitalaltitude} \quad (6.2)$$

For this study though, as the ADCS is of great relevance, a star tracker will be adopted for attitude determination. Its accuracy is substantially better of that of a sun sensor, at a higher economic price of course. The details of a star tracker commercially available online can be found in Table 6.5:

Element: Star tracker	
Parameter	Value
Total mass	250 g
Dimensions	45x50x95 mm
Nominal power consumption	<1 W
Price	30000€
Manufacturer	KU Leuven
Update rate	10Hz
Accuracy (around boresight)	10 arcsec or $2.7 \times 10^{-3}^\circ$ (1-Sigma)
Axis	3

**Table 6.5:** Star tracker attitude sensor parameters

Furthermore, a supplementary sun sensor will be included as a redundant sensor in case the Earth or the Moon get in the field of view of the star tracker:

Element: Digital sun sensor	
Parameter	Value
Total mass	6.5 g
Dimensions	43x14x5.9 mm
Nominal power consumption	0.115 W
Price	3660/euro
Manufacturer	SolarMEMS
Accuracy	<0.5° (3-Sigma)
Axis	2

Table 6.6: Sun sensor parameters

### 6.2.2.2 Attitude actuators

If the attitude of the satellite has suffered from unwanted deviations, its the attitude actuators task to correct it. Besides, they are also used to stop the satellite from detumbling once it has ended the launch phase. Common actuators include magnetorquers or reaction wheels [39].

For this conceptual design, a reaction wheel will be used. Even though it is are heavier than even multiple magnetorquers, reaction wheels provide significantly more torque. Henceforth, stronger disturbance torques (see Table6.4) might be corrected. The reaction wheel actuator though, can cause high frequency jitter (micro-vibrations) that might affect the payload pointing stability. However, such analysis is out of the scope and therefore the jitter effect will be neglected. Next table shows a commercial reaction wheel which fits in the requirements:

Element: Reaction wheel	
Parameter	Value
Total mass	200 g
Dimensions	57x57x31.5 mm
Nominal power consumption	0.180 W
Price	6500€
Manufacturer	CubeSpace
Speed range	±6000 rpm
Speed control accuracy	<5 rpm
Max torque	2.3 mN·m
Momentum storage(at 6000 rpm)	30.0 mN·m·s

Table 6.7: Reaction wheel parameters

Additionally, 3 magnetorquers will be included as complementary attitude actuators. Their torque is much lower, but in case of malfunction of the reaction wheel, the redundancy of attitude actuators could prevent the fatal failure of the mission:

Element: MT01 Magnetorquer	
Parameter	Value
Total mass	7.5 g
Dimensions	50x50x3.2 mm
Nominal power consumption	0.500 W
Price	800€
Manufacturer	EXA
Nominal magnetic moment	0.39 $Am^2$
Angular acceleration (for 1U panel)	3.2 $rad/sec^2$
Torque (for 1U panel)	0.00536 mN·m

Table 6.8: Magnetorquer parameters

### 6.2.3 Communication system

The communication system is in charge of receiving commands from the ground station (receiving phase) and transmitting the payload and housekeeping data down to the ground station (transmitting phase). It is as well responsible of establishing inter-satellite communications, but they will be disregarded.

To transmit the big amount of data that the payload can generate, a high downlink rate is required. It is directly proportional to the transmission frequency. Current commercial high data rate communication products emit and receive in the S-Band with a frequency between 2-4 GHz. However, they also consume a considerable amount of power with regards to CubeSat capabilities (view Figure 2.2). In order to optimize the electrical consumption, the following strategy is adopted.

On one hand, the CubeSat on-board transmitter will be a S-band transmitter with a considerable high data rate. The transmitter will downlink the payload and housekeeping data to the ground station via a S-band compatible antenna. Both components are displayed below:

Element: HSTX S-Band Transmitter	
Parameter	Value
Total mass	100 g
Dimensions	96x90x14.2 mm
Maximum power consumption	5 W
Frequency range	2400-2450 MHz
Maximum data rate	7.5 Mbps
Modulation	QPSK
Price	~8500€
Manufacturer	Clyde Space

Table 6.9: S-Band transmitter parameters

Element: S-Band patch antenna type I	
Parameter	Value
Total mass	64 g
Dimensions	98x98x6.5 mm
Maximum RF output power	4 W
Frequency range	2400-2450 MHz
Gain	8.3 dBi
Price	2500€
Manufacturer	EnduroSat

Table 6.10: S-Band antenna parameters

Making the conservative assumption that the satellite will be available for ground station communications around 5min per orbit, the transmitter data rate will allow a total data down-link of 600 MB, equivalent of 1875 images.

On the other hand, receiving commands from the ground station does not require such high data rate, so cheaper and less power demanding products can be used. A UHF transceiver -primarily configured as a receiver- and a UHF antenna will be enough for the receiving phase:

Element: UHF Transceiver type II	
Parameter	Value
Total mass	94 g
Dimensions	96x90x14.2 mm
Maximum power consumption (Tx/Rx)	1 W / 0.082 W
Frequency range (Tx/Rx)	400-403 MHz / 430-440 MHz
Maximum data rate	7.5 Mbps
Modulation	2GFSK
Price	3500€
Manufacturer	EnduroSat

Table 6.11: UHF transceiver parameters

Element: UHF deployable antenna	
Parameter	Value
Total mass	85 g
Dimensions (undeployed)	98x98x12.1 mm
Maximum RF output power	3.5 W
Frequency range	435-438 MHz
Gain	>0 dBi
Price	3000€
Manufacturer	EnduroSat

Table 6.12: UHF antenna parameters

A more strict communication system design would assess the several transmitting and receiving output/input powers, the antenna gains and the Signal-to-Noise ratios to finally come out with a link budget. As stated in Section 5.1.5, it will not be evaluated in this project.

### 6.2.4 Command and Data Handling system

This system is responsible of validating, decoding and distributing received ground station commands to other satellite systems, as well as gathering, preparing and storing payload and housekeeping data for communication downlink (in this CubeSat design though, the payload will be stored automatically in the mass storage of 160GB). Ultimately, the system also monitors the satellite health [21].

The system is generally composed an on-board computer including a nanocontroller with mission flight control software and data storage components. In this design, the flight computer will not need to high storing capabilities as the payload will be automatically stored in its own mass storage of 160 GB. A suitable commercial command and data handling computer can be:

Element: On-board computer	
Parameter	Value
Total mass	70 g
Dimensions	96x90x10 mm
Maximum power consumption	0.2 W
nanocontroller	32-bit ARM Cortex-M3-based MCU
Memory	4 MB
Communication	I2C / CAN / UART
Price	4500€
Manufacturer	CubeSpace

Table 6.13: On-board computer parameters

Additionally, usual CubeSat commercial mission flight control software cost around 20,000€.

### 6.2.5 Thermal control system

The main task of the thermal system is to determine the temperature of all the satellite systems and subsystems and maintain them in the optimal secure operational range. The thermal control of a CubeSat can either be done by passive or active methods. In active control methods, the battery thermometer sensor continuously checks the temperature whereas a heater regulates it. Passive control methods rely on the idea that the heat sources from the satellite (electrical power dissipated, heat due to propulsion system, thermal emission) are balanced out by the external heat sources (direct solar radiation, solar radiation reflected from the Earth, Earth thermal radiation, etc.).

In this design, a passive thermal control system will be approached. It will be considered that the high area to volume ratio will prevent the systems from overheating while the heat generated by the propulsion system will keep the CubeSat warm in the eclipse phase. Furthermore, thermal variations in VLEO are not as extreme as in higher orbits.

### 6.2.6 Propulsion system

Propulsion systems in satellites are generally used for 4 different purposes:

- Orbit maintenance. Depending on the orbit conditions, satellites might require a propulsion system to keep them in the desired orbit.
- Orbit change and other manoeuvres. It is not quite frequent, but some satellites might need their own on-board propulsion system to autonomously change orbit inclination or achieve any other sort of singular manoeuvres that were typically done by a rocket.

- Precise attitude control. Some propulsion systems, for e.g. the ion engines, can offer very precise yet relatively strong thrust and impulse bits. This is of vital importance to big satellites but it can also be useful for constellations of formation flying CubeSats or fractionated spacecraft (see Section 2.1).
- De-orbit. As mentioned in Section 4.1, all new satellites must re-enter within 25 years. Therefore, when drag is not strong enough, a propulsion system is required to bring the satellite down to Earth.

In the case of this conceptual CubeSat design, the nano-propulsion system IFM will be used to fully compensate drag and maintain, as long as possible, the desired VLEO. Although the engine has its own lifetime cap, it is expected that the limiting factor will be the mass of propellant that the CubeSat can carry on-board. In the IFM case, the propellant mass is already determined by the manufacturing company, and the amount of solid propellant included in each engine seems that can not be changed.

The properties of the IFM nano-thruster can be found in the next table:

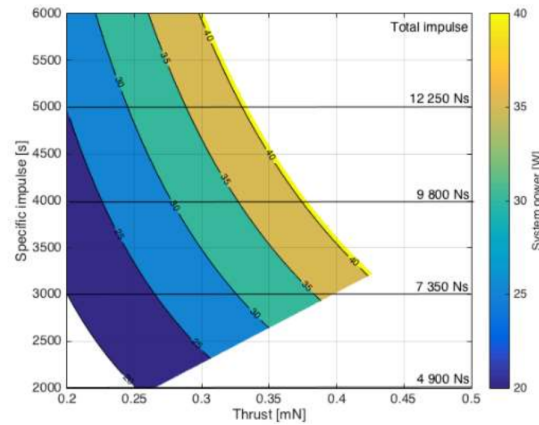
Element: IFM Nano Thruster	
Parameter	Value
Engine type	FEET
Total mass (dry)	670 g
Propellant	Indium (solid fuel)
Propellant mass	250 g
Dimensions	100x100x82.5 mm
Dynamic thrust	0.010 mN to 0.4 mN
Nominal thrust	0.35 mN
Specific impulse	2000-6000 s
Total power range	8-40 W
Power at nominal thrust	40 W
Nominal P/T	114.29 W/mN
Lifetime	17000 h
Price (including fuel)	40,000€
Manufacturer	FOTEC / Enpulsion

Table 6.14: IFM nano-thruster parameters

From Table 6.14 and as stated in Section 5.1.3, it can be detected that the IFM thruster provides a really high specific impulse, better than any other nano-propulsion. But it comes at the cost of low maximum thrust and high power-to-thrust ration. At CubeSat scale, even low thrust may prove enough to compensate drag at VLEO, at least the higher VLEO orbits. It is the power-to-thrust ratio that is more concerning for such small satellites. However, the IFM engine does not require to operate at full power consumption. Indeed, the engine can work in a big envelope of power consumption as a function of thrust or specific impulse provided: In fact, propulsion systems used in many bigger satellites are conceived to operate in on-off mode for a fixed level of thrust and their duty cycle is adjusted to keep the desirable orbit while saving fuel [25]. In VLEO though, the orbital decay is so quick that the extra thrust that the thruster should provide to recover the nominal orbit is not worth it, so engines operate in a quasi-continuous state [33]. Furthermore, high frequency of on-off cycles could sometimes prematurely degrade the engine. For simplicity reasons, in the conceptual design of this CubeSat it is going to be assumed that the engine operates constantly.

As with any conventional propulsion system, the IFM engine is composed of 3 elements: the thruster itself, the tankage and the propellant. At the same time, the tankage consists of the





**Figure 6.1:** IFM nano-thruster relation between specific impulse, thrust and power consumption

propellant tank, the feed systems (which brings the propellant from the tank to the thruster) and the required control hardware. The *Expulsion* company sells the entire engine, with all three elements already assembled together.

### 6.2.7 Electric power system

Being one of the most important systems, the electrical power system has to supply enough power for the entire satellite platform through all its lifetime. The system consists of a power source, energy storage, Power Distribution Unit (PDU) and other power regulation elements. The most common power source of CubeSats are photo-voltaic solar cells while the energy storage is usually done by batteries.

In this study, the electric power system will be designed using a maximum power consumption approach. This is to say that the system has to be characterised according to the End of Life (EOL) maximum power requirements. Therefore, to properly size the electric power system, the rest of the satellite systems and subsystems have to be set into maximum power consumption, even if it is not needed to. For example, at the specified orbit of 250km, the IFM engine will not operate at maximum thrust or power conditions, but it will be assumed so. This criteria will allow for the characterisation of the maximum capabilities that a 6U CubeSat can offer currently.

In the case of an EO CubeSat, it can be deduced that the power requirements will change according to four different operational modes: imaging, eclipse, downlink and battery recharge:

In imaging, the payload will be at imaging mode and the S-Band transmitter and antenna (transmitting subsystem) will be off. In eclipse, the payload will be at off mode and the transmitting subsystem will be off too, but the solar arrays will not be active so the required power will be supplied from the batteries. In downlink, the payload will be off but the S-Band transmitter and antenna will be on, thus considerably increasing power consumption. Finally, in battery recharge, the payload will be in read-out mode and the transmitting subsystem off again. The ADCS, the UHF transceiver and UHF antenna (receiving subsystem), the propulsion system and the command and data handling system will be powered at all time. The power consumed by the PDU can be neglected.

Table 6.15 shows the summarised power budget consumption for every system in each operational mode (for systems with variable power configurations, the maximum power setups have been selected). The power needed to recharge the batteries is yet To Be Determined (TBD):



System / Mode	Imaging (W)	Eclipse (W)	Downlink (W)	Battery Recharge (W)
Payload system	3.5	0	2.5	0
ADCS	2.8	2.8	2.8	2.8
Communications	3.6	3.6	12.6	3.6
Command and data handling	0.2	0.2	0.2	0.2
Propulsion system	40	40	40	40
Electric power system	$\sim 0$	$\sim 0$	$\sim 0$	*TBD
Total power consumption	50.1	46.6	58.1	46.6

**Table 6.15:** CubeSat summarised power budget for the several operation modes (without battery power consumption determined) and the IFM-design case

In eclipse mode, the batteries will have to provide 46.6 W. Considering that eclipse will last for 35.74 min, the total energy that must be delivered to the CubeSat during eclipse will be 27.75 Wh. A suitable commercial battery for this study could be:

Element: Pegasus Class BA01/D	
Parameter	Value
Total mass	180 g
Total dimensions	89x95x14 mm
Energy storage	44.4 Wh
Nominal supply power	3.7 V
Nominal supply current	12000 mAh
Number of cells	8
Price*	5800€
Manufacturer	Exa

**Table 6.16:** Battery parameters

As it can be concluded, the most demanding mode will be battery recharge, due to the high electric power demands of the CubeSat and all the conservative assumptions. Therefore, the battery recharge mode will be used for the overall electric power system sizing and in the later results as maximum power consumption mode.

Then, assuming that imaging time is 1 min and downlink will last for 5 min, the remaining sun-light time available for battery charging is 47.61 min (see Table 5.1). Then, assuming a 90% recharge efficiency, the power consumption required to fully recharge the batteries in 47.61 min is 38.86 W. Those 38.86 W are added in the battery charge power consumption for a total of 85.46 W. Finally, adding a 15% safety margin leads to a total maximum power consumption of 98.28 W. However this is the EOL required power, so to properly size the solar arrays the Beginning Of Life (BOL) power should be found. Current solar arrays of satellites at about 500 km degrade at a 3% rate per year [16]. To be conservative, a 10% yearly degradation due to atomic oxygen will be assumed at 250km. Then, taking into account that the CubeSat EO mission described in this study will last for around a year, it can be concluded that the minimum BOL power generation should be 109.19 W, a tremendously high amount for 6U CubeSat standards (see Figure 2.2).

The only commercially available solar array for 6U CubeSats capable of such power generation is manufactured by *dhv technology*. It is a deployable Triple Junction GaAS solar array formed by 2 wings of 3 solar panels per wing:

Element: BCT 6U Solar Panel	
Parameter	Value
Total mass	300 g
Total dimensions	360x189.5x1.6 mm
Solar array power	20 W
Bus voltage	7-23 VDC
BOL efficiency	29.5% / 1267 W/m <sup>2</sup>
Price*	8600€
Manufacturer	dhv technologies

Table 6.17: Single BCT 6U solar panel parameters

Element: BCT 6U-H Triple Wing Solar Array	
Parameter	Value
Total mass	<1800 g
Total dimensions	360x189.5x4.8 mm each wing
Solar array power	120 W
Bus voltage	7- 23 VDC
BOL efficiency	29.5% / 1267 W/m <sup>2</sup>
Price*	51600€
Manufacturer	dhv technologies
Number of panels	6 (2x3)

Table 6.18: BCT 6U-H Triple Wing Solar Array parameters

\*The price of the total solar array was not available online, but similar commercial 6U deployable solar panels can be bought for 8600€. The solar array will provide extra 8.33 W, so there is even more power supply margin.

## 6.3 Overall CubeSat system configuration

Now that the entire CubeSat systems have been explained, sized and selected, a review of its characteristics as a whole platform will be done. Again, it will be part of a conceptual design. Mechanical, structural, thermal, optical analysis and testing should be done in order to optimize the overall CubeSat performance.

### 6.3.1 Total mass budget

Once all the different systems and subsystems of the CubeSat are assembled together the total mass budget accounting for the mass of all the systems and subsystems of the CubeSat can be made:

Element	Mass (g)
6U Structure	1100
Payload system	1350
Chameleon Imager (+storage)	1350
ADCS	479
Star Tracker	250
Sun sensor	6.5
Reaction Wheel	200
Magnetorquer (x3)	22.5
Communication system	343
S-Band transmitter	64
S-Band antenna	100
UHF Transceiver (Rx)	94
UHF antenna	85
Command and data handling	70
Computer	70
Propulsion system (dry)	670
IFM Nano Thruster	670
Electric power system	1980
BCT 6U-H Triple Wing Solar Array	1800
Pegasus Class BA01/D	180
Dry mass	5992
Propellant	250
Wet mass	6242
15% Margin	899
Total mass	6891

**Table 6.19:** Mass budget for the CubeSat design using an IFM engine

It can be seen that the entire CubeSat mass is 6.89 kg, below the maximum allowed total mass for 6U CubeSat satellites, according to CDS (see Table 2.2). However, it has to be taken into account that this result is due to the fact that the propellant mass is already fixed at 250g by the provider of the IFM thruster. Such low fuel amount is going to be the limiting factor of the mission lifetime in orbit. Nonetheless, an improved version of the IFM CubeSat design could be done employing the spare mass for extra fuel storage, greatly increasing the time in orbit. The spare mass could also be used, totally or partially, to add extra payload instruments, increasing the potential income generated by the satellite.

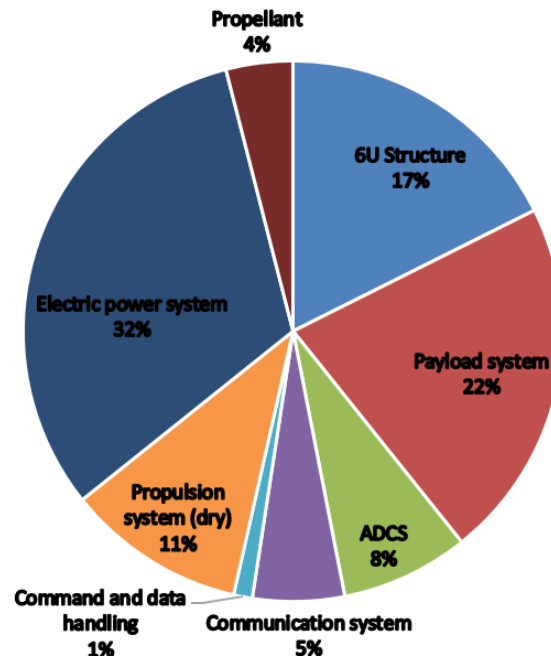


Figure 6.2: Relative mass distribution for CubeSat design using an IFM engine

From the relative mass distribution in this CubeSat configuration it can be surprisingly noticed that the heavier subsystem is not the propulsion one, but rather the electric power system. This is due to low thrust-to-power ratio of the IFM engine, which requires a massive amount of solar cells to supply enough power in order to operate. This fact is so remarkable that in this setup the electric power system mass (1.98kg) doubles the total propulsion system mass (920 kg).

### 6.3.2 Total power budget

Once the power supply required for each CubeSat system has been acquainted, the power budget can be presented, either in an absolute way or in a relative way with regards to the different systems. It has to be reminded that the CubeSat has 4 possible operating modes:

System / Mode	Imaging (W)	Eclipse (W)	Downlink (W)	Battery Recharge (W)
Payload system	3.5	0	2.5	0
ADCS	2.8	2.8	2.8	2.8
Star Tracker	1	1	1	1
Sun sensor	0.12	0.12	0.12	0.12
Reaction Wheel	0.18	0.18	0.18	0.18
Magnetorquer (x3)	1.5	1.5	1.5	1.5
Communication system	3.58	3.58	12.58	3.58
S-Band transmitter	0	0	5	0
S-Band antenna	0	0	4	0
UHF Transceiver (Rx)	0.08	0.08	0.08	0.08
UHF antenna	3.5	3.5	3.5	3.5
Command and data handling	0.2	0.2	0.2	0.2
Propulsion system	40	40	40	40
Electric power system	0	0	0	38.86
Power consumption	50.08	46.58	58.08	85.44
15 % Margin	7.512	6.987	8.712	12.816
Total power consumption	57.59	53.57	66.79	98.26

Table 6.20: Power budget for the CubeSat design using an IFM engine

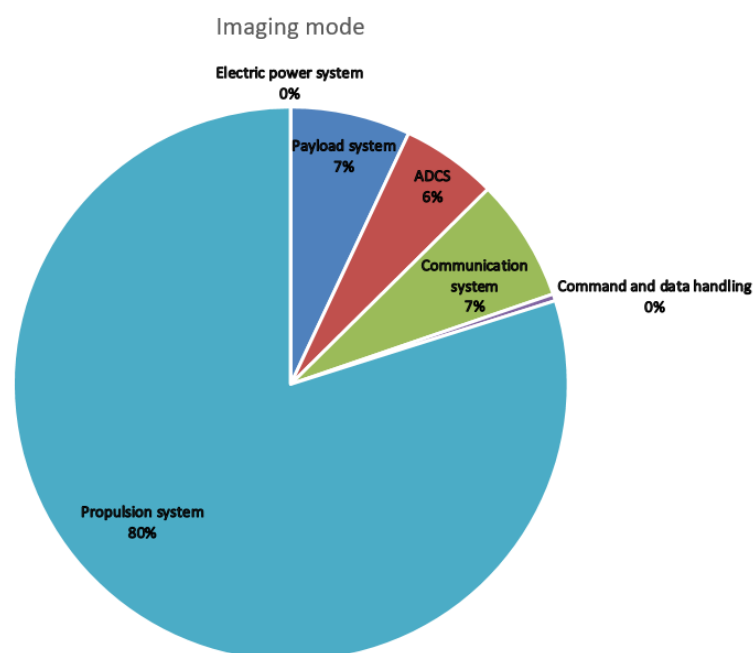
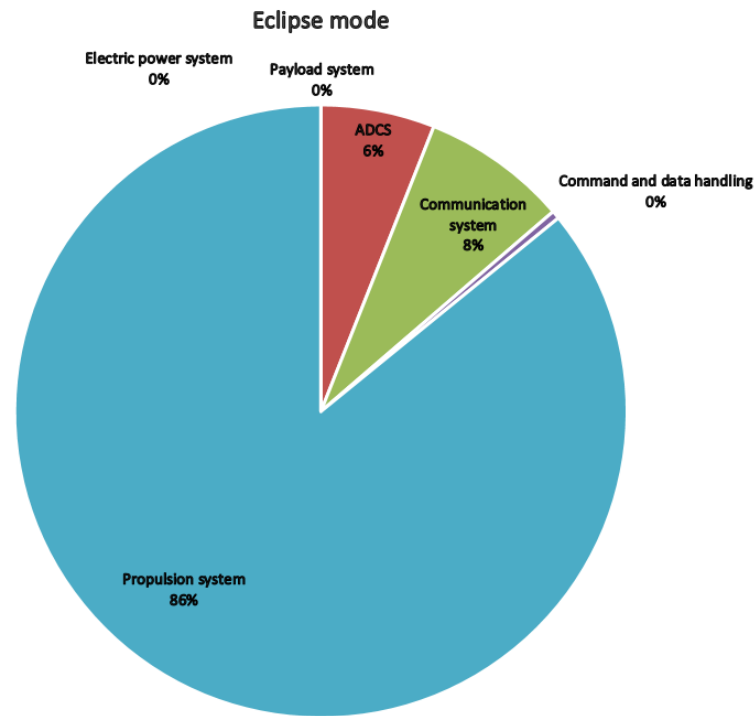
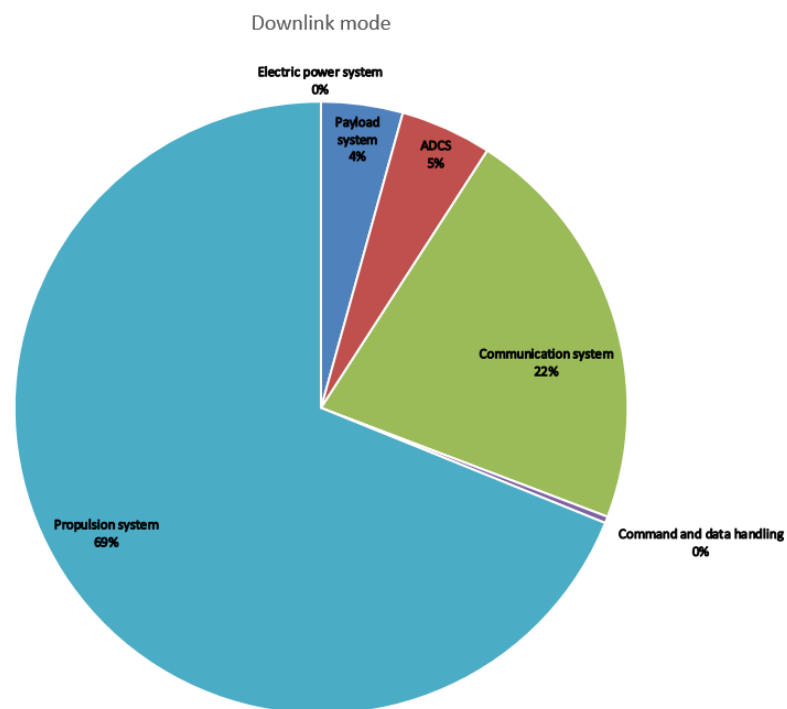


Figure 6.3: Relative power consumption in imaging mode for the IFM CubeSat design



**Figure 6.4:** Relative power consumption in eclipse mode for the IFM CubeSat design



**Figure 6.5:** Relative power consumption in downlink mode for the IFM CubeSat design

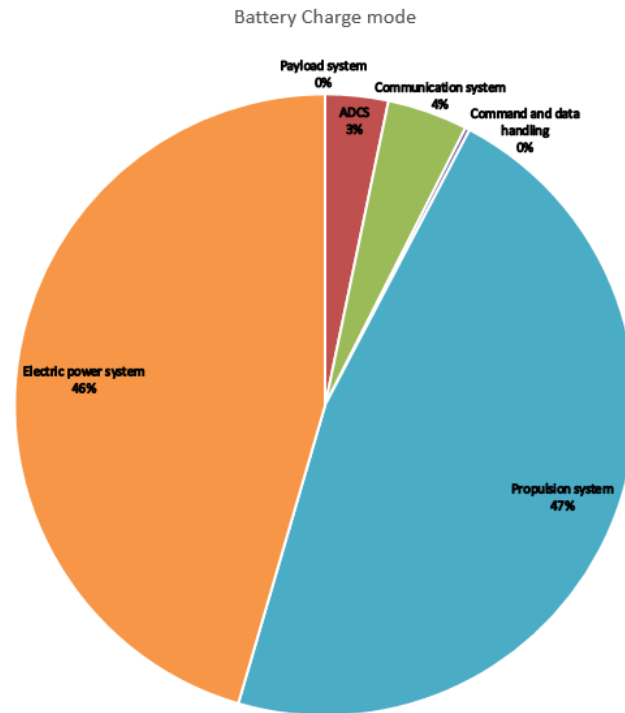


**Figure 6.6:** Relative power consumption in battery recharge mode for the IFM CubeSat design

From the total power budget it can be noticed how impacting the propulsion system power consumption is, as it drains the major part of the power supply available (around 80%) in imaging and eclipse operation modes. However, it is the battery recharge mode that is the most restricting one in terms of power consumption, as it practically doubles the power consumption in regards of the other three operation modes.

It has to be noted that even in the battery recharge mode, the power supply will provide an surplus of 21,74 W. This spare amount of power supply could be used to decrease the battery recharge time.

This power budget proves that the overall high power consumption will become a real challenge in the design of electric thrusted CubeSats in any kind of mission in the VLEO range.

### 6.3.3 Total element budget

If all the different element prices are accounted together, the total element cost of a single CubeSat using this IFM engine configuration can be obtained. This resulting element cost indicates how much expensive buying all the different parts of the CubeSat would be. It is not to be confused with the total manufacture unit cost, as this should take into account the assembly costs, the determination of which is out of the scope of this project.

Element	Price (€)
6U Structure	7850
Payload system	116000
Chameleon Imager (+storage)	116000
ADCS	42560
Star Tracker	30000
Sun sensor	3660
Reaction Wheel	6500
Magnetorquer (x3)	2400
Communication system	17500
S-Band transmitter	8500
S-Band antenna	2500
UHF Transceiver (Rx)	3500
UHF antenna	3000
Command and data handling	24500
Computer+software	24500
Propulsion system (wet)	40000
IFM Nano Thruster + Propellant	40000
Electric power system	57400
BCT 6U-H Triple Wing Solar Array	51600
Pegasus Class BA01/D	5800
Net cost	305810
15 % Margin	45871.5
Total mass	351681.5

Table 6.21: Element budget for the CubeSat design using an IFM engine

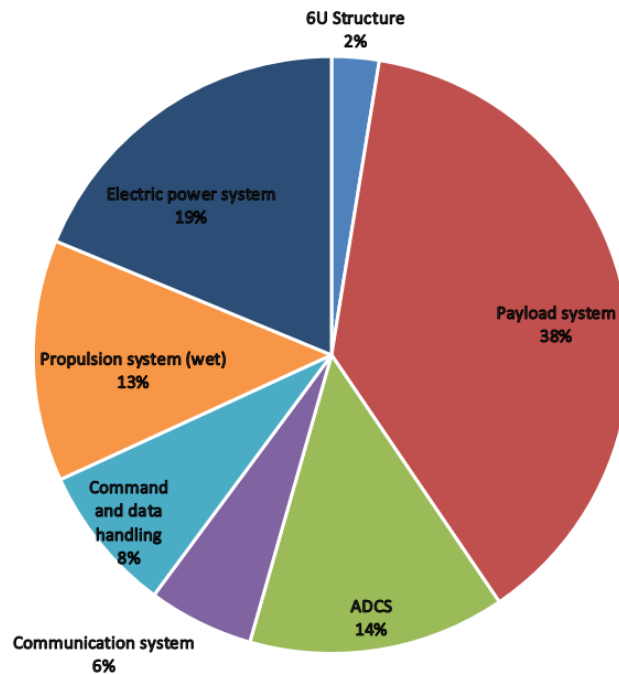


Figure 6.7: Relative cost distribution for CubeSat design using an IFM engine

Unlike the mass and power budgets, the element manufacture budget is shaped by the payload system. This is due to the high resolution camera that composes the system. As beforehand stated, such a quality camera setup has been chosen in order to provide commercially competitive imagery. However, the impact in the CubeSat element budget, although useful



in regard to possible high quality payload setups for EO missions at VLEO, should not be given much importance as it is not a critical element of the CubeSat critical design.

It is much more relevant noticing that, concerning the other CubeSat systems, the costs of the electric power system plus the costs of the propulsion system make up for a total of almost one third of the entire CubeSat element manufacture cost, up to almost 100,000 euros. Such high increase in the manufacturing costs drifts apart from the CubeSat standard key elements (simple and cheap components, see Section 2.1).

This indicates that perhaps the CubeSat platform is not currently suitable for VLEO environment, as the propulsion system required for continuous orbit maintenance stretches to the limit the already mince nano-satellite capabilities. This is to say that nowadays the power supply required for VLEO operation is so high that such region is more convenient for bigger more capable satellites.

#### 6.3.4 CubeSat design conclusions

Here concludes the conceptual design and sizing of a CubeSat carrying a miniature IFM engine. It has been proved that a CubeSat configuration carrying a conventional propulsion system could be constructed.

Despite the fact that initially seemed that it's design was going to be restricted by the propulsion system available mass, it turned out that the most critical system design is going to be the electrical power unit, either by mass limitations or by maximum power available. The significantly high power consumption for the proper operation of the propulsion systems as drag compensations systems will pose a challenge in the design of any thrusted CubeSat operating at VLEO.

As stated in Chapter 5, this was just a preliminary sketch, proposed under several assumptions. It is by no means a definitive functional design as a more meticulous technical analysis and further testing ought to be done.

## Chapter 7

# CubeSat design using ABEP approach

In this chapter, the conceptual design for an EO CubeSat orbiting at VLEO developed in Chapter 6 will be rethought. This time, the CubeSat will carry an ABEP system, the AB-GIE conceived at the University of Colorado, for full drag compensation [15]. In this case though, it must be taken into account that most of the ABEP technologies are still in early development phases, so many characteristics of them are not available or are just predictions. Again, this new design will take the assumptions and statements of Chapter 5 as guidelines. Many of the several systems adopted in the previous chapter can be reused in this design. This is due to the fact that the two engines, the IFM nano-thruster and the AB-GIE, both have in common a singular design driver parameter: really high power-to-thrust ratio that is severely restricted by CubeSats power constraints (see Figure 2.2). Moreover, making both conceptual designs similar will allow for a more impartial and non-biased comparison.

### 7.1 Structural architecture

Starting with the architectural framework, it is unclear how the AB-GIE nano-engine will fit inside the 6U CubeSat traditional chassis. Regarding Figure 5.3, the presence of an AB engine inside a nano-satellite might lead into a volume problem. For the simplicity of this study, such issue will not be considered.

### 7.2 Systems and subsystems

The following systems and its adopted commercial components will be identically replicated from the previous design:

- Payload system. Same optical *Chameleon* RGB panchromatic camera, including the 160GB mass storage.
- Communication system. One could think that the S-Band modules could be removed to save power during downlink mode, at the cost of way lower data rates. Nonetheless, the results of the FEED design have demonstrated that it will be pointless as the most power demanding phase is battery recharge. Moreover, the downlink phase is completely supplied with solar array power.
- Thermal propulsion system. Once again, it will be assumed that the high area to volume ratio will prevent the systems from overheating while the heat generated by the propulsion system will keep the CubeSat warm during eclipse.

- Command and Data Handling system. Spite the fact that the higher operating complexity of AB-GIE systems may require more robust software (and therefore hardware), it will be considered that the on-board computer characteristics will stay practically the same.

The rest of the systems have been reshaped to fit with the new CubeSat design:

### 7.2.1 Propulsion system

Obviously, the engine change has significantly modified the propulsion system essence. As in the case of the IFM thruster design, the purpose of the propulsion system in this mission is to generate enough thrust to compensate drag and henceforth maintaining the desired orbit as long as possible. In the IFM example, the limiting factor was supposed to be the amount of on-board propellant. In this case, the time in orbit will be determined by the AB-GIE lifetime, influenced by the cathode degradation due to atomic oxygen erosion [7].

As the AB-GIE engine is still in preliminary design, many of its parameters are not available (N/A) yet, whereas many other parameters are just theoretically predicted. The following table shows performance obtained by the University of Colorado AB-GIE thruster, along with similar AB-GIE engines (see Section 2.3):

Element: Air-Breathing Gridded Ion Engine (AB-GIE)	
Parameter	Value
Discharge type	DC
Propellant	Residual atmospheric constituents (AO,O <sub>2</sub> ,N <sub>2</sub> )
Diameter	< 9cm
Total mass (dry)	N/A
Dynamic thrust range	>0.001 mN to <0.1 N (highly depends on altitude and power)
Nominal thrust	N/A
Specific impulse	>3000s
Power range	N/A
Power-to-thrust ratio (P/T)	~35 W/mN
Ionization efficiency	0.1-0.5
Thruster efficiency	N/A
Lifetime	10000 h

Table 7.1: AB-GIEparameters

Furthermore, the performance of its pertinent air-intake:

Element: parabolic air-intake for AB-GIE	
Parameter	Value
Inlet radius	5 cm
Exit radius	1 cm
Length	10 cm
Capture efficiency	>0.5

Table 7.2: AB-GIE parabolic air-intake

From Table 7.1, it can be seen that the total mass of the engine has yet to be obtained, as well as its operating power ranges. The estimation of the maximum value that these parameters can get for a 6U CubeSat will eventually be done.

### 7.2.2 ADCS

The operating regime of the AB-GIE is likely to enlarge the disturbance torques described in Table 6.4. Although the characterisation of the aerodynamic and propulsive disturbance torques is out of the scope of this project, a second reaction wheel actuator will be used to account for the possible increase in unwanted torques. The new reactive wheel will have the same attributes than the original wheel.

### 7.2.3 Electric power system

The new design of the electric power system will be done in a similar way than in the previous design. Again, a maximum power consumption approach will be considered. Nonetheless, in Section 6.2.7 it was deduced that by imposing a maximum power criteria, the power that the solar arrays would be required to supply would be humongous. As the proposed *BCT 6U-H Triple Wing Solar Array* is the only commercially available solar array capable of providing such power, it will also be the adopted solar array for this design.

For the new conditions of this design, a new power budget for each operating modes has to be done:

Where  $MP$  is the maximum power that can be supplied to the propulsion system and  $MB$  is the power that will need to be provided to fully recharge the batteries. From the power budget power consumption relations and knowing the sunlight and eclipse orbital, the following system of equations can be extracted:

$$6.78 + MB + MP = 120 * 0.9 * 0.85 \quad (7.1)$$

$$\frac{1}{0.9} * (6.78 + MP) * 35.74 = MB * 47.61 \quad (7.2)$$

The first equation stands for the maximum power that the solar arrays can produce at battery charge mode considering EOL conditions and including a 15% power margin (the 0.9 and 0.85 factors respectively). The second equation represents the energy that the batteries will spend in eclipse mode (left) with relation to the energy that can be given to the batteries during battery recharge mode, accounting for a 90% recharge efficiency too. Resolving the system of equations, it can be concluded that the maximum power that an the AB-GIE could use in such conditions is 44,43 W. Therefore, according to the T/D of Table 7.1, the maximum thrust that the AB-GIE can produce in such conditions is 1.23 mN, 3 times higher than the maximum possible thrust of the IFM engine (0.4 mN).

Besides, the power that is needed to refill the batteries in recharge mode is 43.27 W. The energy that the batteries have to deliver in eclipse mode is 30.50 Wh, so the battery cells used in the previous design are still valid for this setup.

The procedure to calculate the maximum available mass for the AB-GIE engine can be done in a similar way. Assuming that the CubeSat has the maximum permissible mass of 8 kg, contemplating the 15% margin and knowing that the structure and other CubeSat systems (accounting for the extra reaction wheel) have a mass of 5522g. The result of such calculation is that the AB-GIE engine in this CubeSat configuration can have a mass up to 1434g. It might seem enough regarding that AB-GIE do not carry propellant nor any sort of tankage, but it has to be taken into account that the obtained mass includes the thruster itself but also the air-intake inlet.

### 7.3 Overall CubeSat system configuration

Now that the entire CubeSat systems have been explained, sized and selected, a review of its characteristics as a whole platform will be done.

#### 7.3.1 Total mass budget

Unlike the IFM CubeSat design, in this case the propulsion system total mass was unknown, so it has been estimated the maximum available mass that the AB-GIE could have (1.434 kg). This mass is higher than the total wet mass of the IFM propulsion unit. Considering that no fuel storage system will be required, this mass would be able to compensate for the robust AB-GIE structure, see Figure 5.3.

Element	Mass (g)
<b>6U Structure</b>	<b>1100</b>
<b>Payload system</b>	<b>1350</b>
Chameleon Imager (+storage)	1350
<b>ADCS</b>	<b>679</b>
Star Tracker	250
Sun sensor	6.5
Reaction Wheel (x2)	400
Magnetorquer (x3)	22.5
<b>Communication system</b>	<b>343</b>
S-Band transmitter	64
S-Band antenna	100
UHF Transceiver (Rx)	94
UHF antenna	85
<b>Command and data handling</b>	<b>70</b>
Computer	70
<b>Propulsion system</b>	<b>1434</b>
ABIE	1434
<b>Electric power system</b>	<b>1980</b>
BCT 6U-H Triple Wing Solar Array	1800
Pegasus Class BA01/D	180
<b>Dry mass</b>	<b>6956</b>
<b>15 % Margin</b>	<b>1043</b>
<b>Total mass</b>	<b>8000</b>

**Table 7.3:** Mass budget for the CubeSat design using an AB-GIE engine

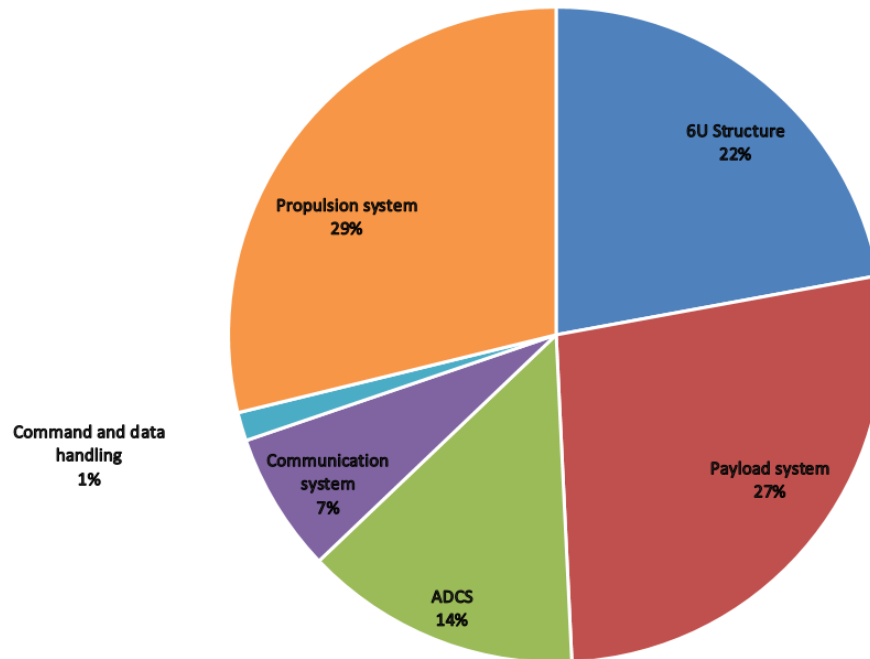


Figure 7.1: Relative mass distribution for CubeSat design using the AB-GIE

### 7.3.2 Total power budget

Again, the electric power that the AB-GIE engine would consume at maximum operation regime is not yet experimentally determined, so the highest power that it could consume has been estimated accounting for the most critical CubeSat operation mode (battery recharge). Such maximum power consumption is quite similar to the one of the IFM propulsion system. Nonetheless, the higher thrust-to-power ratio of the AB-GIE system will allow to provide much higher thrust than the IFM.

System / Mode	Imaging (W)	Eclipse (W)	Downlink (W)	Battery Recharge (W)
Payload system	3.5	0	2.5	0
ADCS	2.98	2.98	2.98	2.98
Star Tracker	1	1	1	1
Sun sensor	0.12	0.12	0.12	0.12
Reaction Wheel(x2)	0.36	0.36	0.36	0.36
Magnetorquer (x3)	1.5	1.5	1.5	1.5
Communication system	3.58	3.58	12.58	3.58
S-Band transmitter	0	0	5	0
S-Band antenna	0	0	4	0
UHF Transceiver (Rx)	0.08	0.08	0.08	0.08
UHF antenna	3.5	3.5	3.5	3.5
Command and data handling	0.2	0.2	0.2	0.2
Propulsion system	44.43	44.43	44.43	44.43
Electric power system	0	0	0	43.47
Power consumption	54.69	51.19	62.69	94.66
15 % Margin	8.2035	7.6785	9.4035	14.199
Total power consumption	62.8935	58.8685	72.0935	108.859

Table 7.4: Power budget for the CubeSat design using an AB-GIE engine

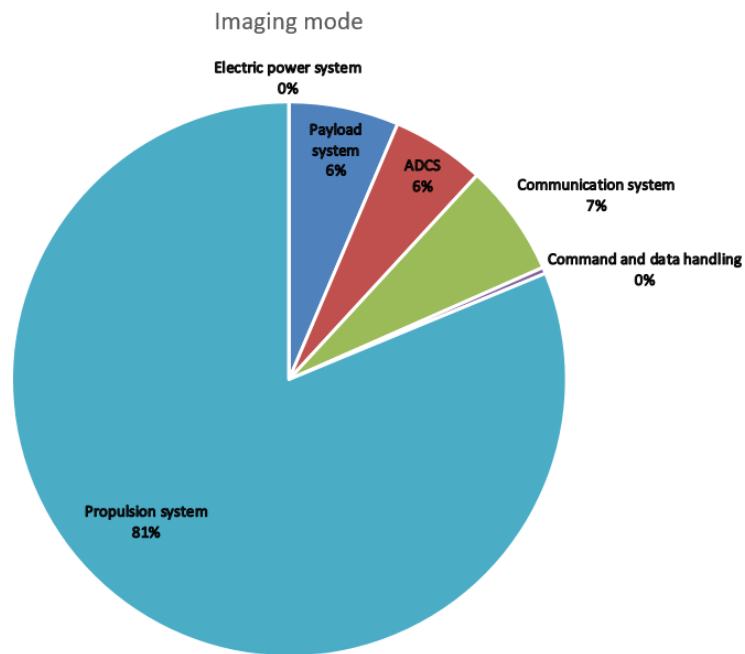


Figure 7.2: Relative power consumption in imaging mode for the AB-GIE CubeSat design

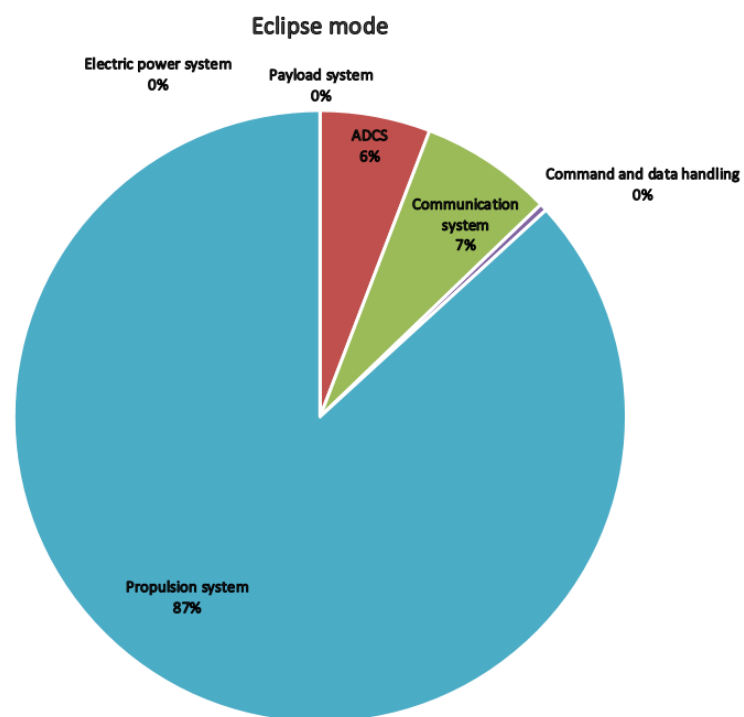
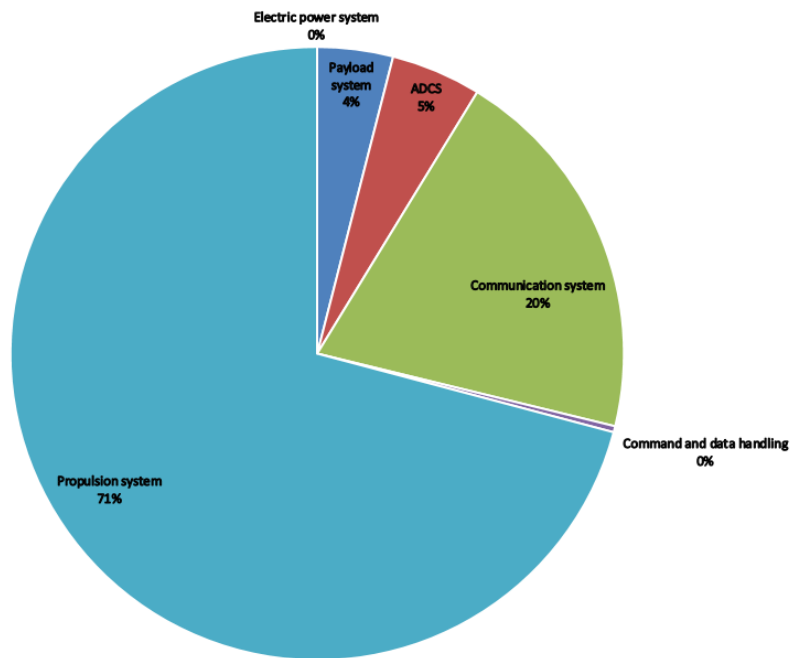
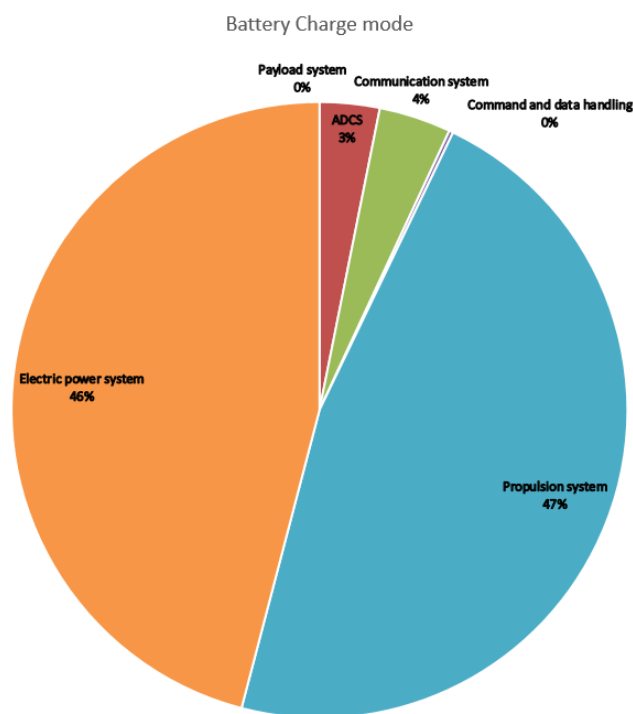


Figure 7.3: Relative power consumption in eclipse mode for the AB-GIE CubeSat design



**Figure 7.4:** Relative power consumption in downlink mode for the AB-GIE CubeSat design



**Figure 7.5:** Relative power consumption in battery charge mode for the AB-GIE CubeSat design

### 7.3.3 Total element budget

For the third time, the AB-GIE budget parameter is still unknown. In this case though, the maximum possible price that the AB-GIE could have can not be properly estimated. However, both the AB-GIE system costs plus the electrical power unit costs will probably lead to a considerable increase in the manufacturing costs of the complete CubeSat, just like in the IFM CubeSat design.



Element	Price (€)
6U Structure	7850
Payload system	116000
Chameleon Imager (+storage)	116000
ADCS	49060
Star Tracker	30000
Sun sensor	3660
Reaction Wheel(x2)	13000
Magnetorquer (x3)	2400
Communication system	17500
S-Band transmitter	8500
S-Band antenna	2500
UHF Transceiver (Rx)	3500
UHF antenna	3000
Command and data handling	24500
Computer+software	24500
Electric power system	57400
BCT 6U-H Triple Wing Solar Array	51600
Pegasus Class BA01/D	5800
Net cost	272310
15 % Margin	40846.5
<b>Total element manufacture cost</b>	<b>313156.5</b>

**Table 7.5:** Element manufacture budget for the CubeSat design using an AB-GIE engine

### 7.3.4 CubeSat design conclusions

Here concludes the conceptual design and sizing of a CubeSat carrying a miniature AB-GIE system. It has been proved that a CubeSat configuration carrying an ABEP could be constructed.

Again, the most critical design factor has been the total power consumption. However, it has been found out that the AB-GIE does not have much maximum available mass. Therefore, depending on the total mass that the AB-GIE does finally get, there could be a mass problem in this configuration.

Overall, both IFM and ABEP CubeSat designs have become quite similar. This is due to the fact that both configurations were selected for the exact same mission in the exact same conditions. Furthermore, both propulsion systems have quite resembling characteristics.

## Chapter 8

# CubeSat propulsion system performance analysis

Now that the conceptual designs of the 2 different CubeSat configurations have been presented and compared, its time to compare the performance that each engine would have in VLEO conditions, always taking into account the assumptions in Section 5.1.5.

### 8.1 Drag force determination

First of all, the actual drag force received by the satellite shall be obtained. Taking into account the assumptions made in Section 5.1.5, the drag force can be calculated as shown in Eq. 8.1:

$$F_D = \frac{1}{2} A \rho C_D V^2 \quad (8.1)$$

First of all, the total density of the residual atmosphere species must be found. To do so, it can be simulated using the JB-2006 atmospheric model from the European Corporation for Space Standardization [11]. As mentioned in Section 3.1.3, this is the most accurate model regarding the total density of the residual atmosphere.

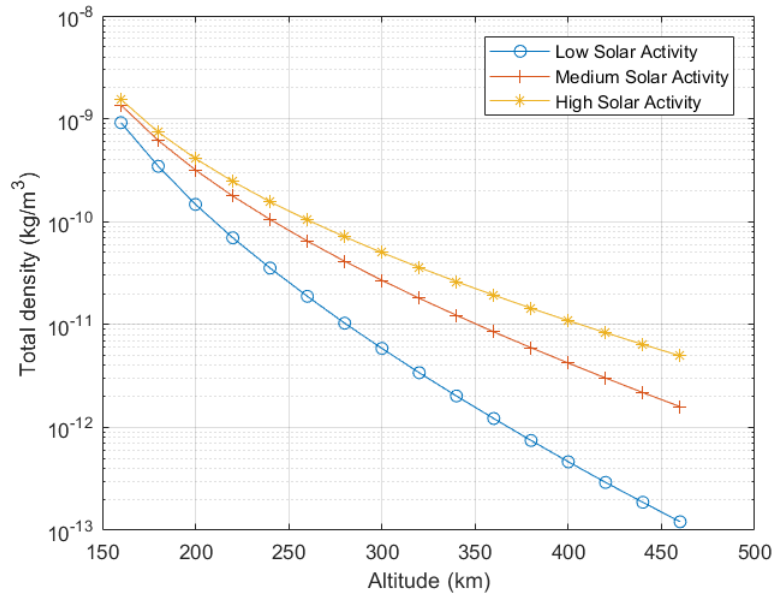


**Figure 8.1:** total atmospheric density as a function of altitude and for different levels of solar activity

As it can be observed, at really low orbits the total density is not heavily influenced by the

solar activity, but as the altitude increases the it has a higher influence over the total density. This means that in the lowest orbits the propulsion systems' performance will not depend much on the solar activity but it will progressively do when the altitude increases.

Another parameter that has to be calculated is the relative velocity between the CubeSat and the atmospheric particles. Again, for simplifying purposes it will be considered that the thermal velocity of the atmospheric species can be neglected and that such speed will be equivalent as just the spacecraft velocity, which can be calculated as follows:

$$V_o = \sqrt{\frac{\mu}{R + r}} \quad (8.2)$$

The meaning of each term is explained in Section 5.1.1. Using Eq.8.2 we can plot the satellite's velocity over altitude:

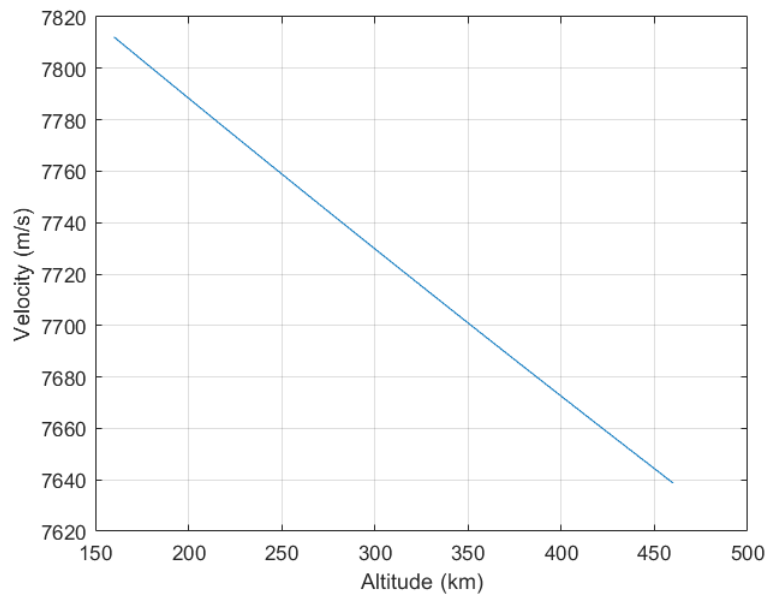


**Figure 8.2:** CubeSat's velocity a function of altitude

Then, the cross-sectional area has already been found of  $0.02m^2$  in Section 5.1.5. Finally, the current literature stipulates that the drag coefficient for conventionally shaped satellites is around  $C_D = 2.2$  [7].

Therefore, the drag force that the 6U CubeSat (in either of both configurations) is going to experience when orbiting at VLEO can be seen at Figure 8.3:

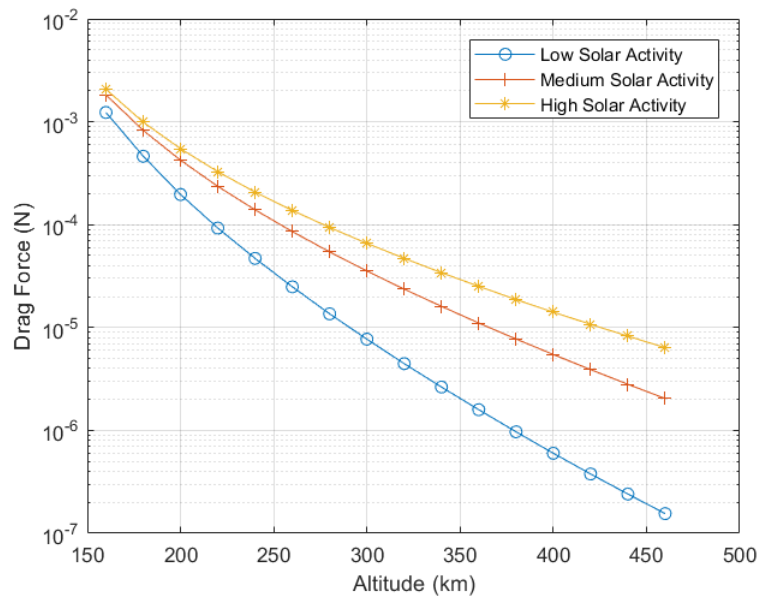


**Figure 8.3:** Drag force as a function of altitude and solar activity

The magnitude of this drag force is the exact amount of thrust that each propulsion system has to provide in order for full drag compensation. If more thrust is provided, the orbit of the CubeSat will rise. In this case, the amount of drag experienced will decrease so the orbit will rise even more and faster. It is not a particularly dangerous situation: if the original orbit was to be recovered, the CubeSat could simply generate less thrust and progressively descend till the desired orbit. This is a particularly interesting strategy if the propulsion system is to operate using a Duty Cycle.

On the other hand though, if the CubeSat generates less thrust than the required in Figure 8.3, the orbit will rapidly decay. Such event can be quite serious if unwanted, as there will be an orbit in which drag force will get bigger than the maximum available thrust so the satellite will de-orbit inevitably. Nonetheless, the same event can be used to effortlessly de-orbit the CubeSat once its active lifetime has expired.

## 8.2 Propulsion operating altitude range determination

However, both IFM nano-thruster and AB-GIE propulsion systems will not be able to provide full drag compensation in all of the VLEO range.

In the case of the IFM thruster there will be a minimum altitude below which drag force will always be greater than the maximum available thrust provided by the engine.

Concerning the AB-GIE system, there will be both a minimum altitude but also a maximum altitude. Again, the minimum altitude will be determined by the maximum available thrust. Nonetheless, the maximum available altitude or ceiling will depend on the minimum possible propellant required for a proper engine operation, see Section 2.3. Such maximum ceiling is expected to be at 600 km for 6U CubeSats[15]:

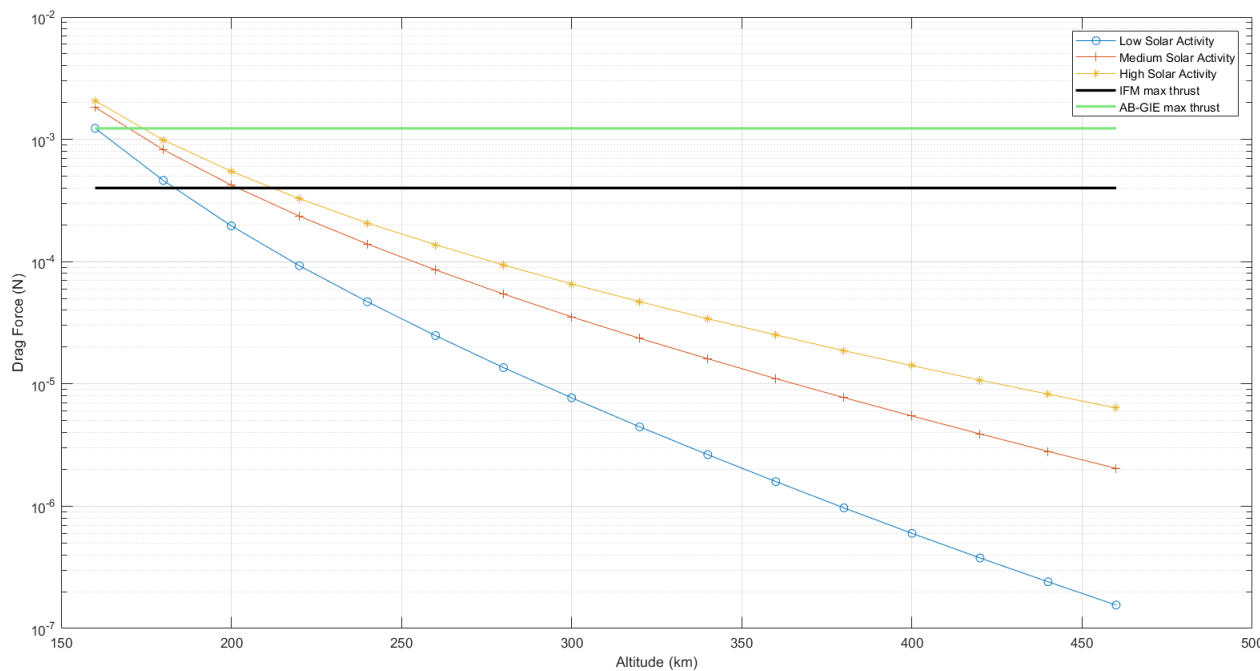


**Figure 8.4:** Maximum available thrust for each propulsion system and its correlation to the drag force as a function of altitude and solar activity

From Figure 8.4, the minimum operating altitudes can be attained by finding the intersection points between the maximum available thrust for each engine and drag force as a function of altitude:

	Low Solar Activity	Medium Solar Activity	High Solar Activity
Minimum altitude (km)	160.1	168.3	172.5
Maximum altitude (km)	600	600	600

**Table 8.1:** Minimum and maximum operating altitude of the AB-GIE system

	Low Solar Activity	Medium Solar Activity	High Solar Activity
Minimum altitude (km)	194.6	203.2	215.9
Maximum altitude (km)	-	-	-

**Table 8.2:** Minimum and maximum operating altitude of the IFM system

### 8.3 Propulsion system operating lifetime

The most important parameter of both engines performance is the period of time that they will actively operate or, in other words, the amount of time that they will be able to maintain the desired orbit, thus heavily deciding the overall mission lifetime.

On one hand, as mentioned in Section 2.3, the operating restraining factor for the AB-GIE is the system electrode corrosion due to AO, which severely reduces its total lifespan. Such lifespan is expected to be round 10000 hours, or **1 year and 51 days**.

On the other hand the operating lifetime of the IFM propulsion system can either be limited by the IFM own lifespan (17000h) or by running out of fuel. In order to determine so, the

following Equation can be used [25]:

$$m_p = \frac{24 * 365 * t * f_D}{Isp * g_0} \quad (8.3)$$

Where  $M_p$  is the total fuel mass,  $t$  is the operating lifespan in hours,  $f_D$  is the drag force compensated by the engine,  $Isp$  is the specific impulse and  $g_0$  is  $9.81m/s^2$ . It should be noted that the specific impulse depends both on the IFM power consumption and on the amount of thrust provided (see Figure 6.1). The determination of the actual operating lifespan can be done assuming for 3 possible scenarios: best possible scenario, nominal scenario and worst possible scenario:

Case	Isp(s)	Thrust(mN)	Supply power (W)	Operating lifespan (h)
Best	6000	0.3	40	5599.32
Nominal	4500	0.35	40	3599.56
Worst	2000	0.25	20	2239.73

**Table 8.3:** IFM operating lifespan for the 3 different scenarios

As it can be seen, in every scenario the IFM operating lifespan will be determined when the engine runs out of fuel. Moreover, even in the best possible scenario, the IFM maximum operating lifespan is still lower than the AB-GIE lifespan.

It must be taken into account that these computes are made considering that the maximum fuel mass is 250g. Nonetheless, in the IFM CubeSat design there was a spare mass of 1.11kg that could be almost entirely used to store extra fuel. Making the computes again with the extra fuel mass the following updated IFM operating lifespan can be obtained for the different scenarios:

Case	Isp(s)	Thrust(mN)	Supply power (W)	Operating lifespan (h)
Best	6000	0.3	40	30236.30
Nominal	4500	0.35	40	19437.62
Worst	2000	0.25	20	12094.52

**Table 8.4:** IFM operating lifespan for the 3 different scenarios and taking advantage of the spare mass

Now, it can be observed that in all three different scenarios the IFM operation lifespan has become greater than the AB-GIE one. However, it has to be said that for the nominal and best case scenario the maximum lifespan will actually be 17000h, as it will be limited by the own IFM engine lifespan, and not the fuel mass available.

## Chapter 9

# Environmental analysis

The development of this bachelor's thesis has been entirely theoretical and analytical. All of the obtained data has been acquired via electronic research or via simulation using software. None of the propulsion systems or the several CubeSat configurations have been actually recreated nor tested physically. Therefore, there is no need for an analysis of the environmental repercussions of this project.

Nonetheless, it is worth noting that the development of the ABEP technologies are environmentally friendly as they do not consume any kind of fuel but instead only require of electrical power supply, which can be gathered using just solar cells. Furthermore, they could even replace some traditional satellite propulsion systems which use toxic fuels such as cesium or hydrazine [25].

## Chapter 10

# Conclusions

After the development of both CubeSat design configuration, its subsequent comparison and result analysis, this project has disclosed some interesting points. It has proved that the critical design factor for thrusting CubeSat EO missions at VLEO is not the maximum available total mass -as it could have seem in the beginning- but rather the maximum available supply power. This is due to the relatively low thrust-to-power ratio that many propulsion systems have, including ABEP technologies. This leads to the overwhelming challenge to stretch the already restrictive CubeSat power supply to a borderline limit (The most powerful solar arrays were required for a proper operation of the satellite systems). Such drawback is balanced out by the significantly high specific impulse that electric propulsion systems have nowadays, which leads to a low fuel consumption.

As well, the project has shown that both the two presented CubeSat configurations, both AB-GIE technologies and conventional electric propulsion systems are capable of providing full drag compensation for a determined VLEO altitude range. The minimum altitude was lower for AB-GIE systems thus allowing for lower orbits but it had a maximum altitude. Instead, the IFM engine had a higher minimum altitude but it does not have a ceiling, so the CubeSat can go as high as desired. It can get above the VLEO range if needed, increasing its mission flexibility.

Moreover, this thesis has found that the operational lifetime of the conventional propulsion systems is limited by the on-board stored fuel whereas the ABEP lifetime is limited by the AO corrosion. This feature, favours ABEP thrusters when the amount of carried fuel is considerably low. However, current electrical propulsion systems have already such high specific impulse that their operational lifespan is much likely to be greater than that of ABEP systems, making them a more suitable option as drag compensation systems in VLEO conditions.



# Bibliography

- [1] Timo Wekerle, José Bezerra Pessoa Filho, Luís Eduardo Vergueiro Loures da Costa, and Luís Gonzaga Trabasso. Status and trends of smallsats and their launch vehicles - An up-to-date review. *Journal of Aerospace Technology and Management*, 9(3):269–286, 2017.
- [2] Eviatar Edlerman and Igal Kronhaus. Analysis of electric propulsion capabilities in establishment and keeping of formation flying nanosatellites.
- [3] Towards the Thousandth CubeSat: A Statistical Overview. *International Journal of Aerospace Engineering*, 2019:1–13, 2019.
- [4] Peter C. E. Roberts. Very Low Earth Orbit mission concepts for Earth Observation . Benefits and challenges BIS-RS-2014-37. (January 2016):0–18, 2014.
- [5] Jose C. Pascoa, Odelma Teixeira, and Gustavo Filipe. A Review of Propulsion Systems for CubeSats. page V001T03A039, 2019.
- [6] F. Romano, B. Massuti-Ballester, T. Binder, G. Herdrich, S. Fasoulas, and T. Schönherr. System analysis and test-bed for an atmosphere-breathing electric propulsion system using an inductive plasma thruster. *Acta Astronautica*, 147(January):114–126, 2018.
- [7] Georg Herdrich, Tony Schönherr, Bartomeu Massuti-Ballester, Francesco Romano, and Kimiya Komurasaki. Analysis of Atmosphere-Breathing Electric Propulsion. *IEEE Transactions on Plasma Science*, 43(1):287–294, 2015.
- [8] Geospatial Education Platform. Orbit Eccentricity [Online] available at <https://www.polyu.edu.hk/proj/gef/index.php/glossary/orbit-eccentricity/>.
- [9] Catalog of Earth Satellite Orbits [Online] Available at <https://earthobservatory.nasa.gov/features/OrbitsCatalog/page1.php>, 2009.
- [10] Ronald J Boain. A-B-Cs of Sun-Synchronous Orbit Mission Design 14 AAS / AIAA Space Flight Mechanics Conference. *14th AAS/AIAA Space Flight Mechanics Conference*, pages 1–19, 2004.
- [11] European Space Agency; European Cooperation for Space Standardization. Space engineering Space environment ECSS Secretariat ESA-ESTEC Requirements; Standards Division Noordwijk, The Netherlands. (November), 2008.
- [12] Bruce Banks, Sharon Miller, and Kim de Groh. Low Earth Orbital Atomic Oxygen Interactions with Materials. (August):1–19, 2012.
- [13] Kh.I. Khalil and S.W. Samwel. Effect of Air Drag Force on Low Earth Orbit Satellites During Maximum and Minimum Solar Activity. *Space Research Journal*, 9(1):1–9, 2016.
- [14] Jose Gonzalez del Amo. European Space Agency (ESA) Electric Propulsion Activities. *34th International Electric Propulsion Conference*, 2017.
- [15] Stephen W. Jackson and Robert Marshall. Conceptual Design of an Air-Breathing Electric Thruster for CubeSat Applications. *Journal of Spacecraft and Rockets*, 55(3):632–639, 2017.

- [16] S. R. Tsitas and J. Kingston. 6U CubeSat design for Earth observation with 6-5m GSD, five spectral bands and 14Mbps downlink. *Aeronautical Journal*, 114(1161):689–697, 2010.
- [17] Arash Mehrparvar. Cubesat Design Specification Rev. 13. *California Polytechnic State University Report*, 2014.
- [18] European Union. DISCOVERER PROJECT. *Seriss.Eu*, (649436), 2015.
- [19] International Journal, Remote Sensing, Yong Xue, Chinese Academy, Jie Guang, Chinese Academy, Jianping Guo, Chinese Academy, Meteorological Sciences, Natural Science View, and Yong Xue. Small satellite remote sensing and applications - History , current and future International Journal of Remote. (August 2008):37–41, 2015.
- [20] Chief International Programme. Small satellites : The NewSpace. 2018.
- [21] Armen Poghosyan and Alessandro Golkar. Progress in Aerospace Sciences CubeSat evolution : Analyzing CubeSat capabilities for conducting science missions. *Progress in Aerospace Sciences*, (September):1–25, 2016.
- [22] CubeSats: Tiny Payloads, Huge Benefits for Space Research | Space, 2018.
- [23] Advantages of LEO Orbit | Disadvantages of LEO Orbit.
- [24] Igor Levchenko, Stéphane Mazouffre, Peter J Klar, Shunjiro Shinohara, Jochen Schein, Laurent Garrigues, Minkwan Kim, Rod W Boswell, Christine Charles, Hiroyuki Koizumi, Yan Shen, Michael Keidar, Shuyan Xu, and Francesco Taccogna. Space micropropulsion systems for Cubesats and small satellites : From proximate targets to furthestmost frontiers. 011104(December 2017), 2018.
- [25] Mirko Leomanni, Andrea Garulli, Antonio Giannitrapani, and Fabrizio Scortecci. Propulsion options for very low Earth orbit microsatellites. *Acta Astronautica*, 133:444–454, 2017.
- [26] MIT Bulletin. Air-Breathing Propulsion. (1):1–9, 2007.
- [27] G. Cifali, T. Misuri, P. Rossetti, M. Andrenucci, D. Valentian, and D. Feili. Preliminary characterization test of HET and RIT with Nitrogen and Oxygen. (August):1–16, 2012.
- [28] A. I. Erofeev, A. P. Nikiforov, G. A. Popov, M. O. Suvorov, S. A. Syrin, and S. A. Khartov. Air-Breathing Ramjet Electric Propulsion for Controlling Low-Orbit Spacecraft Motion to Compensate for Aerodynamic Drag. *Solar System Research*, 51(7):639–645, 2017.
- [29] D. Di Cara, J. Gonzalez del Amo, A. Santovincenzo, B. Carnicero Dominguez, M. Arcioni, A. Caldwell, and I. Roma. RAM Electric Propulsion for Low Earth Orbit Operation : an ESA study. *The 30th International Electric Propulsion Conference*, (17-20 September):IEPC–2007–162, 2007.
- [30] Lawrence E. Murr and William H. Kinard. Effects of low earth orbit. *American Scientist*, 81(2):152–165, 1993.
- [31] The Radiation Environment in Low-Earth Orbit. *Radiation Research*, 148(5):S3, 2006.
- [32] TEC-QI. ESA Requirements on EOL De-orbit Technical Day on De-orbit Strategies. *Technical Day on De-orbit Strategies*, (March), 2015.
- [33] David G. Fearn. Economical remote sensing from a low altitude with continuous drag compensation. *Acta Astronautica*, 56(5):555–572, 2005.
- [34] Nanosatellite and CubeSat Database [Online]. Available at <https://www.nanosats.eu>.

- [35] Frank C. Wong. Understanding the revenue potential of satellite-based remote sensing imagery providers. *IEEE Aerospace Conference Proceedings*, 2005, 2005.
- [36] Richard E Wirz. Miniature Ion Thrusters: A Review of Modern Technologies and Mission Capabilities. *34th International Electric Propulsion Conference*, pages 1–11, 2015.
- [37] Paul Lascombes and David Henri. Electric Propulsion for Small Satellites Orbit Control and Deorbiting : The Example of a Hall Effect Thruster. (June):1–13, 2018.
- [38] *Pocket book about JPEG 2000*. isbn: 1011010011.
- [39] Sua Song, Hongrae Kim, and Young-Keun Chang. Design and Implementation of 3U CubeSat Platform Architecture. *International Journal of Aerospace Engineering*, 2018:1–17, 2018.